

Copyright
by
Yucao Tang
2009

**Calibration of Water Content Reflectometer in Rocky Mountain
Arsenal Soil**

by

Yucao Tang, BS

Thesis

Presented to the Faculty of the Graduate School of

The University of Texas at Austin

in Partial Fulfillment

of the Requirements

for the Degree of

Master of Science in Engineering

The University of Texas at Austin

August 2009

**Calibration of Water Content Reflectometer in Rocky Mountain
Arsenal Soil**

**Approved by
Supervising Committee:**

Jorge G. Zornberg, Supervisor

Chadi S. El Mohtar

Dedication

To Mengying.

Acknowledgements

I would like to acknowledge my supervisor, Dr. Jorge Zornberg, for enlightening and guiding me through my MS study. I am thankful for the opportunity he offered me to study and research the TDR technique at University of Texas, Austin. This experience is challenging and rewarding. I would like to thank Dr. Chadi El Mohtar for being the reader of my thesis and giving me technical comments.

I would like to thank my fellow students in the unsaturated soil research group, and professors at UT Austin for meaningful discussions, experienced suggestions, and their professional comments on my research. I would like to especially thank Jeffery Kuhn, Nathan Thompson, and Michael Plaisted for sharing their experience and experimental data while we were exploring the characteristic of unsaturated soils at UT Austin. I would also like to thank Fei Yan for helping me understand the heat dissipating model in soil and construct a simulation.

I would like to express my most sincere gratitude to my parents. Without their understanding, support, and love, the completion of this thesis would not be possible.

Abstract

Calibration of Water Content Reflectometer in Rocky Mountain Arsenal Soil

Yucao Tang, MSE

The University of Texas at Austin, 2009

Supervisor: Jorge G. Zornberg

This paper describes how water content reflectometers (WCRs) were analyzed to develop a calibration equation. Time domain reflectometry (TDR) technique is the most prevalent method in in-situ moisture monitoring; and WCR is a type of low frequency TDR sensors, which is sensitive to soil type. Developing soil-specific calibration and investigating different environmental effects on WCR calibration is important. This study focused on investigation of the soil dry density and temperature effects on WCR calibration in RMA soil. Two series of tests to develop soil-specific calibration with dry density and temperature offset were conducted. Results from testing program showed that WCR response was positive related to volumetric water content, dry density, and temperature. Equations were developed to illustrate the response-density-temperature-moisture relation. Application to a field site was also presented to illustrate the difference

in volumetric water contents obtained by using manufacturer method and the calibration procedure drawn in this paper.

Table of Contents

List of Tables	xi
List of Figures	xii
Chapter 1: Introduction.....	1
1.1 Research Motivation	1
1.2 Research Objectives.....	3
1.3 Thesis organization	4
Chapter 2: Monitoring Moisture in Soil	6
2.1 Overview.....	6
2.2 The definitions of water content and conventional monitoring method	6
2.3 Monitor Moisture in soil using TDR technique	7
2.3.1 TDR and soil moisture	7
2.3.2 TDR Overview.....	8
2.3.3 Classic Universal Calibration Equation: Topp’s Equation	12
2.3.4 Influence of Soil Type	13
2.3.5 Influence of Soil Density	16
2.3.6 Influence of Temperature and freeze/thaw	17
Chapter 3: Materials and Instrumentations.....	20
3.1 Geotechnical Classifications of Soil	20
3.2 Compaction Curve	22
3.3 The WCR Reflection Calibration System overview	23
3.4 Water Content Reflectometer: WCR CS-616.....	24
3.5 Soil Containers.....	26
3.6 Soil Compaction System.....	27
3.7 Temperature Control System	28
3.8 Data Acquisition System.....	35
Chapter 4: Experimental Procedures	37
4.1 Overview.....	37

4.2	Tests for calibrating WCR with different soil relative compactions ...	37
4.2.1	Basic philosophy and assumptions	37
4.2.2	Testing scope and testing procedures	38
4.3	Tests for calibrating WCR in varied Temperatures	43
Chapter 5:	Effects of Relative compaction on WCR Calibration Curves	46
5.1	Overview and a typical result	46
5.2	Summary of WCR calibration results.....	49
Chapter 6:	Effects of Temperatures on WCR Calibration Curves	56
6.1	Overview and a typical result	56
6.2	Summary of WCR calibration results.....	58
Chapter 7:	Interpretation of WCR Calibration Curves	62
7.1	Overview.....	62
7.2	Interpretation of WCR Response Curves.....	62
7.2.1	Independent fit	62
	Quadratic Regressions:	63
	Cubic Regressions:.....	64
	Linear Regressions:.....	66
7.2.2	Consolidated fit and shift.....	68
	Quadratic regression:	69
	Cubic regression:	71
	Prediction of shift value for other densities:	73
7.3	Interpretation of Temperature Correction Equations.....	74
7.4	Synthesized application of response calibration and temperature correction	81
Chapter 8:	Applications of Calibration Results	83
8.1	Overview	83
8.2	Comparison between the Response Curve in the study and Manufacturer's Response Curve	83
8.3	Comparison between the Temperature Correction Curves in the study and Manufacturer's Temperature Correction	85

8.4 Applications of the Temperature Correction	87
Chapter 9: Summary and Conclusions	90
9.1 Summary of Research Objectives	90
9.2 Conclusion of Reflection Calibration Results.....	92
9.2.1 Conclusion of WCR Reflection Results under Varied Relative Compactions	92
9.2.2 Conclusion of Temperature Corrections Results	94
9.3 Suggestions for Future Research	95
References.....	97
Vita	99

List of Tables

Table 2.1:	Relation of gravimetric water content and volumetric water content.	7
Table 3.1:	Geotechnical properties of RMA soil	22
Table 5.1:	The setup of experiments	46
Table 5.2:	Data of 75% set	50
Table 5.3:	Data of 80% set	51
Table 5.5:	Data of 85% set	51
Table 5.5:	The volumetric portion of soil particles	54
Table 5.6:	The effect of phase portion change on reflecting period	55
Table 6.1:	Scope of temperature correction testing program	56
Table 6.2:	Results of temperature correction tests	58
Table 7.1:	Quadratic polynomial coefficients and R^2 values	63
Table 7.2:	Cubic polynomial coefficients and R^2 values	65
Figure 7.2:	Cubic Fitting Curves of Different Relative Compactions	66
Table 7.3:	Linear Polynomial Coefficients and R^2 Values	67
Table 7.4:	Coefficients of quadratic consolidated fit and shifts, and R^2 values.	69
Table 7.5:	Coefficients of cubic consolidated fit and shifts, and R^2 values	71
Table 7.6:	Correction parameters (20-40°C)	77
Table 7.7:	Correction parameters (0-20°C)	78
Table 7.8:	Correction parameters (-20-0°C)	79
Table 8.1:	bulk densities and volumetric water contents	83

List of Figures

Figure 2.1: A three-phases diagram of soil	6
Figure 2.2: Operating principle and system components of TDR (O'Connor and Dowding, 1999)	8
Figure 2.3: Nominal pulse TDR (O'Connor and Dowding, 1999).....	9
Figure 2.4: TDR system with cable tester and a 3-rod probe.....	10
Figure 2.6: TDR waveforms and and derivative of data for the coaxial probe in air (Caltaldo et al., 2008).....	12
Figure 2.7: The measured relationship between K_a and v_{mc} for four mineral soils (Topp et al. 1980).....	13
Figure 2.8: Influence of soil type on the correlation of water content and the apparent dielectric constant (O'Connor and Dowding, 1999).....	14
Figure 2.9: The calculated relative apparent permittivity [ϵ_{rel}] as a function of volumetric water content for CS615 sensors in construction sand, Lolalita sandy loam, Searla loam, and Larimer Loam. (Kelleners et al. 2005)	15
Figure 2.10: K_a versus v_{mc} for the three different densities (Pozzato et al., 2008)	17
Figure 2.11: Effect of temperature on ϵ_i for the four soils measured at nearly saturated soil water contents (Seyfried and Murdock, 2004)	18
Figure 2.12: WCR Period as a Function of Soil Temperature for Soil A at Volumetric Water Contents (θ) of 0.06, 0.16, 0.26, 0.33, and 0.41. (Benson & Wang, 2006)	19
Figure 3.1: Particle-size distribution for New RMA soil (Thompson, personal communication)	20
Figure 3.2: Liquid limit (Thompson, 2009, personal communication)	21

Figure 3.3: Standard Compaction Curve of RMA Soil	23
Figure 3.4: Apparatus Arrangement: (1) data acquisition system, (2) water content reflectometer, (3) inserting guide tool, and (4) calibration tube	23
Figure 3.5: CS-616 Water Content Reflectometer	25
Figure 3.6: Calibration Tube: a) Various Components; b) Assembling.....	27
Figure 3.7: Air Piston Hammer	28
Figure 3.8: Experiment Environment.....	29
Figure 3.9: Room temperature and WCR response tested in room.....	30
Figure 3.10: Room temperature records and WCR responses in a cooler.....	31
Figure 3.11: Circuit of temperature control system.....	32
Figure 3.12: Temperature controller.....	33
Figure 3.13: Heating elements and electric power supply	33
Figure 3.14: Freezer: (a) outside; (b) inside	33
Figure 3.15: Flowcharts of temperature control system.....	35
Figure 3.17: Data logger CR1000	36
Figure 4.1: A Prepared Pre-wetted Specimen	41
Figure 4.2: A scheme of a post-wetted specimen.....	41
Figure 4.3: The two-prong path from the top of the specimen.....	42
Figure 4.4: Reflectometer in tube.....	42
Figure 4.5: The arrangement inside temperature control system	44
Figure 5.1: Typical readings from 0 to 110 hrs in RMA soil.....	47
Figure 5.2: WCR responses in dry air	48
Figure 5.3: WCR responses in water	48
Figure 5.4: A specimen after testing.....	49

Figure 5.5: Actual dry density and volumetric water content distribution in the three test sets	50
Figure 5.6: The volumetric water content and time relations at different relative compactions	53
Figure 6.1: WCR responses in a graduate cooling test.....	57
Figure 6.2: The equilibrium and representative response	58
Figure 6.3: WCR responses for different temperatures and soil volumetric water content (2.8%, 11%, 16%, 21%, 27%, and 33%)	60
Figure 6.4: WCR responses for different volumetric water contents and temperature (40, 35, 30, 25, 20, 15, 10, 5, 1, -5, -10, -15, and -20 C)	61
Figure 7.1: Quadratic fitting curves of different relative compactions	64
Figure 7.3: Linear fitting curves of different relative compactions.....	68
Figure 7.4: Curves of quadratic consolidated fit and shifts.....	70
Figure 7.5: The relation of dry density and quadratic polynomial shift.....	71
Figure 7.5: Cubic consolidated fit and shifts.....	72
Figure 7.7: The relation of dry density and cubic polynomial shifts.....	73
Figure 7.8: Temperature correction database: A 3-D view	76
Figure 7.9: Temperature correction effect in temperature of 20-40°C.....	78
Figure 7.10: Temperature correction effect in temperature of 0-20°C.....	79
Figure 7.11: Temperature correction effect in temperature of -20-0°C.....	80
Figure 7.12: volumetric moisture content as a function of temperature with the corresponding reflecting period of 40, 35, 30, 25, 20, and 15ms	82
Figure 7.13: volumetric moisture content as a function of reflecting period in the temperature of 40, 35, 30, 25, 20, 15, 10, 5 and 1°C	82

Figure 8.1: Comparison of the WCR responses results in this study and the manufacturer's equation.....	84
Figure 8.2 Temperature correction comparison (30°C).....	85
Figure 8.3 Temperature correction comparison (15°C).....	86
Figure 8.4 Temperature correction comparison (1°C).....	86
Figure 8.5: An application using manufacturer's temperature correction equation to a field	88
Figure 8.6: An application using the temperature correction in this study to a field	88
Figure 8.7: A sample comparison of two temperature corrections	89

Chapter 1: Introduction

1.1 RESEARCH MOTIVATION

Unsaturated soils have three main components: the soil particles, the air, and the water stored in pores. The hydraulic characteristic of unsaturated soils is usually illustrated by two relationships: water retention curve (WRC), and hydraulic conductivity function (K-function). The WRC describes how water is stored in pore spaces between soil particles; the volumetric water content (θ) and the matric suction in pores are two controlling variables. The K-function describes how the soil particles restrict the water flow through pore spaces; the hydraulic conductivity (k) and the water pressure (h) are two controlling variables. The hydraulic conductivity (k) is usually derived from the changing of volumetric water content (θ). After all, volumetric water content (θ), matric suction, and water pressure (h) are the three key variables which quantify the hydraulic characteristic of unsaturated soil.

Unsaturated soil is very common in geotechnical applications, such as landfill systems, earth dams and embankments, roadway pavements, earth retaining systems, and some foundations. The hydraulic characteristic of these soils is one of the most important engineering aspects, because by knowing the hydraulic characteristic engineers can predict the water movement through the soil, the strength of soil which is related to water content, and the swell/shrink behavior of soil. The hydraulic characteristic of unsaturated soils is also one of the main concerns in agricultural engineering. By quantifying the

hydraulic characteristic, engineers can arrange the water supplies and irrigations for the growing of crops.

Because the hydraulic characteristic is so relevant to many engineering applications, efforts are spent by many researchers on monitoring the three key variables: volumetric water content (θ), matric suction, and water pressure. In the field of monitoring volumetric content, the time domain reflectometry (TDR) technique is being widely and successfully used. As will be presented in Chapter 2, the concept of this technique is based on the measurements of the material dielectric permittivity (K_a) from TDR and a K_a - θ_v calibration curve. However, as also will be discussed in Chapter 2, the response of TDR is affected by many factors, such as the soil type, the density of soil, and the temperature of soil. Using a universal calibration curve in real applications, where these impacting factors are keeping changing, would yield to inadequate understanding of the hydraulic characteristic of soil.

The purpose of this study is to present an experimental approach to calibrate water content reflectometer sensors (a type of TDR sensors) for monitoring volumetric water content (θ). In general, the concept of calibration is checking the responses in various nominal conditions using the same installation method that would be applied in real applications. The nominal condition setups in this study will involve the calibration with different relative compactions (i.e. with different dry densities), and in different soil temperatures.

1.2 RESEARCH OBJECTIVES

The specific research objectives of this study include:

- Determine the effects of water content and dry density on the WCR responses in one temperature, and derive numerical equations which can precisely depict the effects;
- Determine the effects of water content and temperature on the WCR responses with one relative compactions, and derive numerical equations which can precisely depict the effects;
- Compare and validate the water content, dry density and temperature relation with generic curves provided by manufacturer;
- Apply the results to one field sample that use similar soil with the same dry density.

To achieve these objectives, following tasks will be fulfilled:

- Review the terminology for monitoring moisture in soils;
- Review the basic concept of using TDR to monitor moisture in soils;
- Review the yard-stick calibration method of TDR;
- Review the influences of soil type, soil density, and temperature to the application of TDR technique;
- Characterize a soil that is useful for calibration;
- Select and Illustrate the TDR sensors that is useful for calibration;

- Design, verify and arrange the instrumentations of calibration to measure the key variables, time frames and impacting factors that are needed for developing a calibration curve;
- Present a theoretical explanation for the experimental data from the calibration;

1.3 THESIS ORGANIZATION

A review of the basic physics of TDR technique and several important factors which might influence TDR response in soil are presented in Chapter 2. This chapter is used to provide a background of monitoring soil moisture.

The geotechnical characteristic of the soil used in this study is described in Chapter 3. This chapter also includes the instrumentations used in the study to contain soil, to compact soil, to maintain a temperature-constant environment, and to acquire measurements. The experimental procedures are described in Chapter 4. This part includes the procedures for preparing and compacting soil, the procedures for calibrating sensors with different relative compactions, and the procedures for calibrating sensors in different temperatures.

The results of tests conducted with different relative compactions are presented in Chapter 5. The results from sensor calibration in different temperatures are presented in Chapter 6. In these two chapters, typical response-time results, the assumptions and standards adopted to choose representative points, and results in respect to independent factors are presented. Chapter 7 includes an analysis and interpretation of the data from the tests stated in Chapter 5 and 6. Chapter 8 provides a comparison between the results

in this study and the generic equations offered by manufacturer, as well as a sample application of the calibration to a set of data from one field using similar soil profile.

Finally, a summary of how the research objectives stated above were achieved, conclusions generalized from the research, and recommendations for future research are presented in Chapter 9.

Chapter 2: Monitoring Moisture in Soil

2.1 OVERVIEW

In this chapter, a general simplified comprehension of soil structure is presented. Variables derived from this comprehension which quantify the soil moisture, as well as the conventional method for measuring these variables, are also presented. Subsequently, an overview on using TDR technique to measure those variables is provided. This chapter also describes various important factors which might affect the application of TDR.

2.2 THE DEFINITIONS OF WATER CONTENT AND CONVENTIONAL MONITORING METHOD

A three-phase diagram is usually used to illustrate the composition of soil, shown in Figure 2.1. Gravimetric water content (ω), usually know as water content, is defined as the mass of water (M_w) over the mass of soil (M_s). Volumetric water content (θ) is defined as the ratio of volume of water (V_w) to total volume (V). The relation of the two water contents is summarized in Table 2.1.

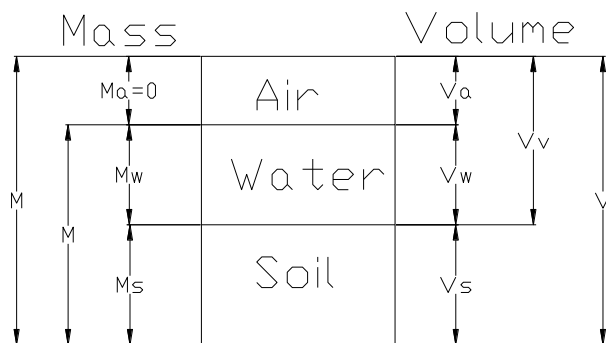


Figure 2.1: A three-phases diagram of soil

Table 2.1: Relation of gravimetric water content and volumetric water content

Variable	Definition	Derivation	Derivation	Derivation
ω	$= \frac{M_w}{M_s}$	$= \frac{\rho_w \cdot V_w}{\rho_d \cdot V}$	$= \frac{\rho_w \cdot \theta}{\rho_d}$	
θ	$= \frac{V_w}{V}$	$= \frac{M_w}{V \cdot \rho_w}$	$= \frac{1}{V \cdot \rho_w} \cdot \frac{\omega}{\omega + 1} \cdot M$	$= \frac{\rho}{\rho_w} \cdot \frac{\omega}{\omega + 1}$

where, ρ_w is the density of water, ρ_d is the dry density of soil specimen, and ρ is the bulk density of soil specimen.

The ω is usually measured directly by oven drying soil samples: first, the weight of wet soil is measured (W_w); subsequently, the wet soil is placed in an oven with the setting temperature over 100°C for 24 hours, so that the water in soil is evaporated; at last, the dried soil is taken out from oven and weighted (W_d), and $\omega = \frac{W_w - W_d}{W_d}$.

The volumetric water content (θ) indicates the storage of water in unsaturated soil. The upper bound value of θ is the same as porosity (n), where $n = V_v/V$. Volumetric water contents can be measured indirectly by TDR travel time.

2.3 MONITOR MOISTURE IN SOIL USING TDR TECHNIQUE

2.3.1 TDR and soil moisture

Time domain reflectometry (TDR) is an electrical measurement technique that is sensitive to the dielectric property of material around. Using TDR to measure soil moisture is effective because water has a significantly different higher dielectric constant (80) among the three phases (air=1, soil particles=4-8). For this reason, the volumetric change of water causes a change of dielectric constant of soil. As a result, TDR, which

responds according to the dielectric property of material, can be applied as an indicator of water in soil.

2.3.2 TDR Overview

TDR is a device that emits an electrical pulse, and scans and records the time of the reflection. Subsequently, the time of reflection is used to calculate the dielectric constant of material.

Figure 2.2 shows a diagram that describes the working process of a TDR system (O'Connor and Dowding, 1999). As can be seen, a time step signal (square wave) is first generated by Pulser; subsequently, the square wave travels along Sampler and the cable tester, and the voltages of wave that travel through and reflect back are recorded; sufficient number of this type of waves are generated over time, and a curve that records the reflection coefficients (reflected voltage over transmitted voltage) and reflecting times is produced. Figure 2.3 shows how the square waves are generated; in this figure, 300mV step pulses are launched in every 200 μ sec (O'Connor and Dowding, 1999).

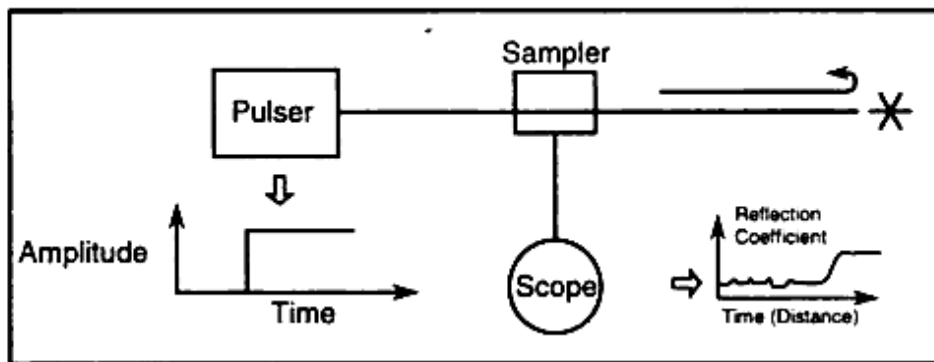


Figure 2.2: Operating principle and system components of TDR (O'Connor and Dowding, 1999)

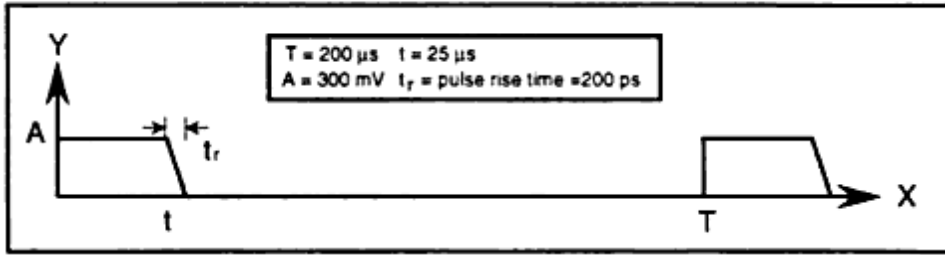


Figure 2.3: Nominal pulse TDR (O'Connor and Dowding, 1999)

Figure 2.4 shows a TDR system for measuring soil moisture used in the geoenvironmental laboratory at UT Austin (TDR 100, manufactured by Campbell Sci., Logan, UT); it contains a three-rod probe, a multiplier, a signal generator and a receiver (cable tester), and a PC. In application, the three-rod probe is inserted into soil; the signal generator generates a fast rise-time voltage step pulse to the cable; the signal travels along the cable till it reaches the rods, at which a portion of the signal is reflected back to the cable tester because of the impedance mismatch that caused by the soil around the rods; a portion of the signal keep propagating through the rods and eventually reach the end of the rods, sending the second reflection to the cable tester. This process is continued until a stable waveform is produced. The waveform would show the time difference between two reflections, and the identification of the two reflections is based on the voltages of them.

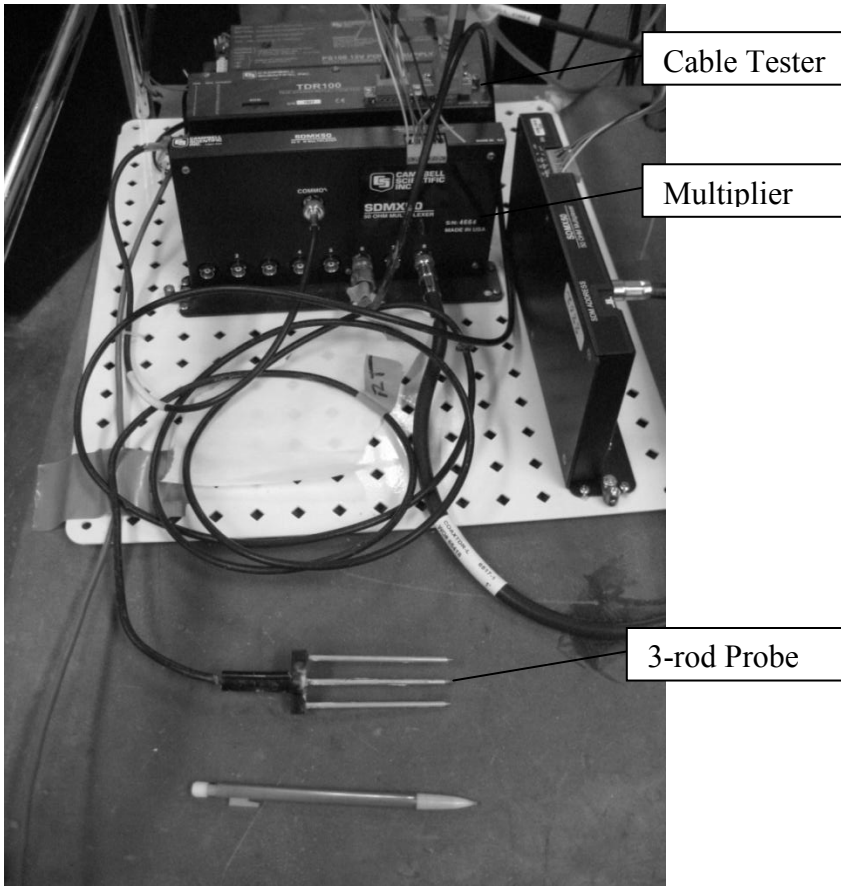


Figure 2.4: TDR system with cable tester and a 3-rod probe

A determination of apparent dielectric constant using a conventional reflection waveform is shown in Figure 2.5; in this figure, voltage versus distance along the probe is displayed (Kim & Benson, 2002). Kim and Benson used a signal with the propagation velocity of c (light speed, $3 \times 10^8 \text{ m/s}$) in cable tester for measuring volumetric water content. When the propagation velocity is c , the apparent length of probe, L_a , is determined from the waveform. Knowing the actual length of probe, the apparent dielectric constant (K_a) is determined:

$$Ka = \left(\frac{La}{Lp}\right)^2 \quad \text{(Equation 2.1)}$$

A TDR calibration is to determine the $La-\theta_v$ relationship, by testing La in soil specimens in different volumetric water contents (θ_v).

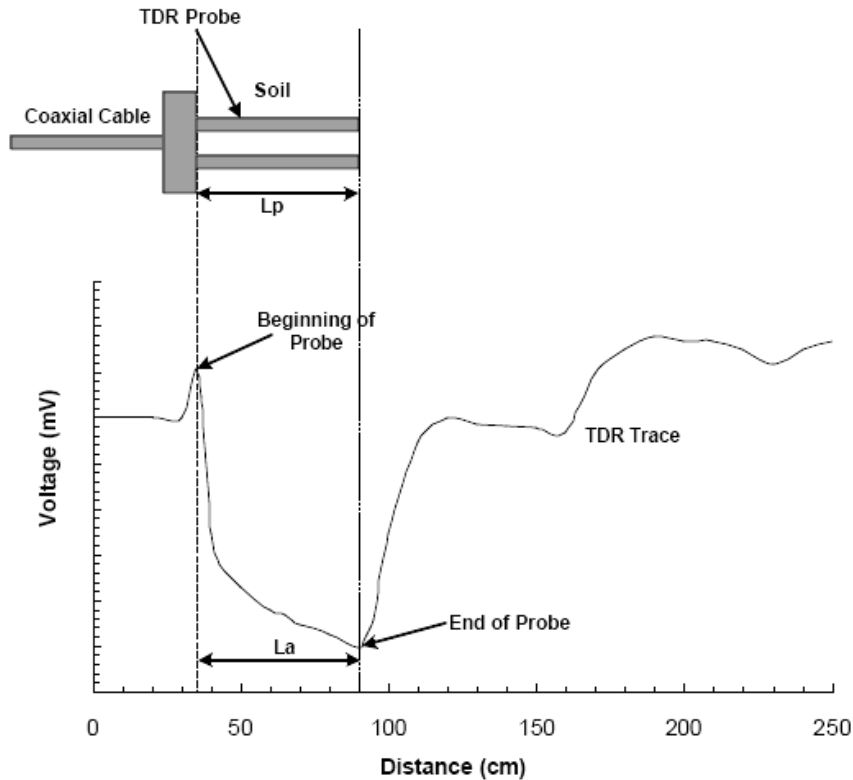


Figure 2.5: TDR waveform analysis. Distance based $V_p=c$ (Kim & Benson, 2002)

The identification of reflections usually uses a derivative method, as illustrated in Figure 2.6. In this figure, the first derivative of the reflecting waveform is plotted (Caltaldo et al., 2008). As can be seen, the start of probe is selected at the first peak of the derivative curve, and the end of probe is selected at the third peak (highest peak) of the derivative curve which is also the point of inflexion of the reflecting curve. The point of

inflexion is correlated to the location of the maximum energy of wave (McCartney, 2007).

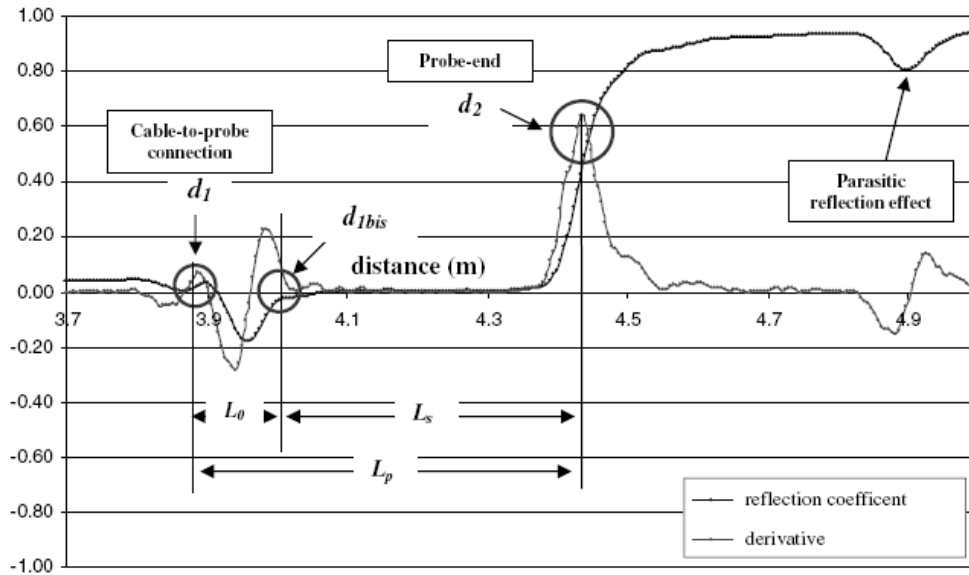


Figure 2.6: TDR waveforms and derivative of data for the coaxial probe in air (Caltaldo et al., 2008)

2.3.3 Classic Universal Calibration Equation: Topp's Equation

In order to relate the TDR measurements and volumetric water contents in soil, a $Ka-\theta_v$ calibration is required. In 1980, Topp et al. stated a calibration equation for mineral soils, based on their experimental results on nine mineral soils, shown in Figure 2.7. They thought this equation was sufficient and would not yield significant difference between soil types. This calibration is widely used nowadays as a universal calibration and known as Topp's Equation:

$$\theta = 4.3 \times 10^{-6} \cdot Ka^3 - 5.5 \times 10^{-4} \cdot Ka^2 + 2.92 \times 10^{-2} \cdot Ka - 5.3 \times 10^{-2}$$

(Equation 2.2)

This empirical finding promoted the application of TDR technique significantly, and made it a standard technique for monitoring water content in field (Friedman et al. 2006).

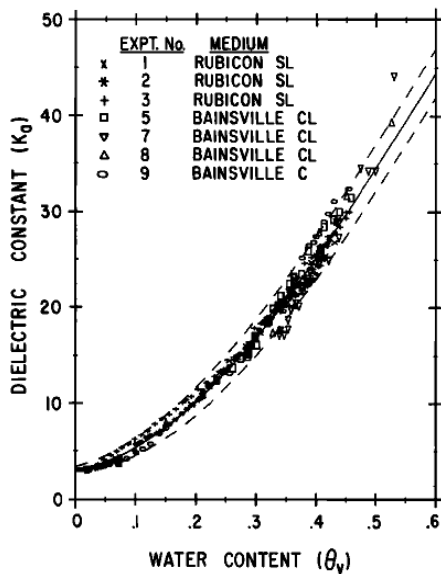


Figure 2.7: The measured relationship between K_d and θ_v for four mineral soils (Topp et al. 1980)

2.3.4 Influence of Soil Type

Pure water has a dielectric constant of 80 at 20°C; however, the dielectric constant of soil particles varied from less than five to ten. Moreover, the dielectric constant is a parameter defined macroscopically, which is defined as the ratio of the stored electrical energy when a potential is applied on a material, to the energy when the potential is applied on vacuum. That means some microscopic changes of soil particles, such as changes of shape, quantity in unit space, orientation, and arrangement, might affect the amount of energy stored in given space, leading to a change of apparent dielectric

constant. Therefore, examining the TDR responses in soil-specific way is inevitable (Petersen, 1995).

Bohl and Roth summarized a K_a and volumetric water content (θ) relation, based on 418 sets of results, each set contained three samples. These soil samples were classified, according to their texture, organic content, and porosity. The relation is shown in Figure 2.8 (O'Connor and Dowding, 1999). As can be seen, organic soils generally have smaller apparent dielectric constant at the same volumetric water content.

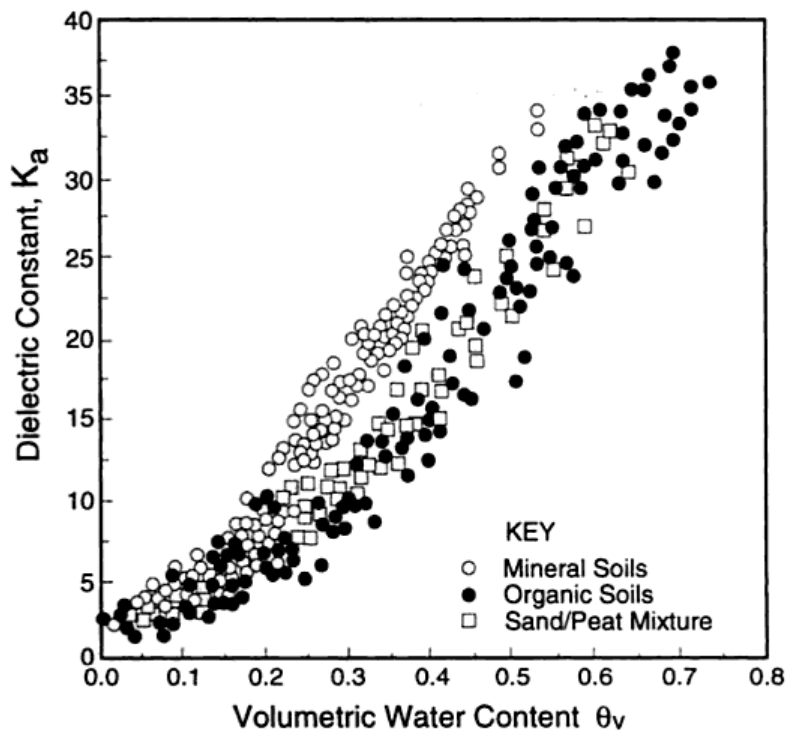


Figure 2.8: Influence of soil type on the correlation of water content and the apparent dielectric constant (O'Connor and Dowding, 1999)

Kelleners et al. (2005) stated that the non-zero electrical conductivity (EC) of soil increased the imaginary part of permittivity, and hence apparent dielectric constant. This

effect might not be negligible in wet saline soils with high clay content. Additionally, electrical conductivity increased the attenuation of the electromagnetic pulse, so that the triggering of the next pulse was delayed. This delay led to an increase of estimated travelling time, hence a higher apparent dielectric constant value.

The apparent dielectric constant and volumetric water content relation using a low frequency TDR (WCR CS615) for four soils, including construction sand, Lolalita sandy loam, Searla loam, and Larimer Loam, is shown in Figure 2.9. As can be seen, only the construction sand (no clay, electrical conductivity=0) matches Topp's Equation satisfactorily. This finding might indicate that: Topp's equation might be only adequate to be applied in non-clayey soil; low frequency TDR is more sensitive to soil type than conventional sensors, using a universal calibration might be unrealistic.

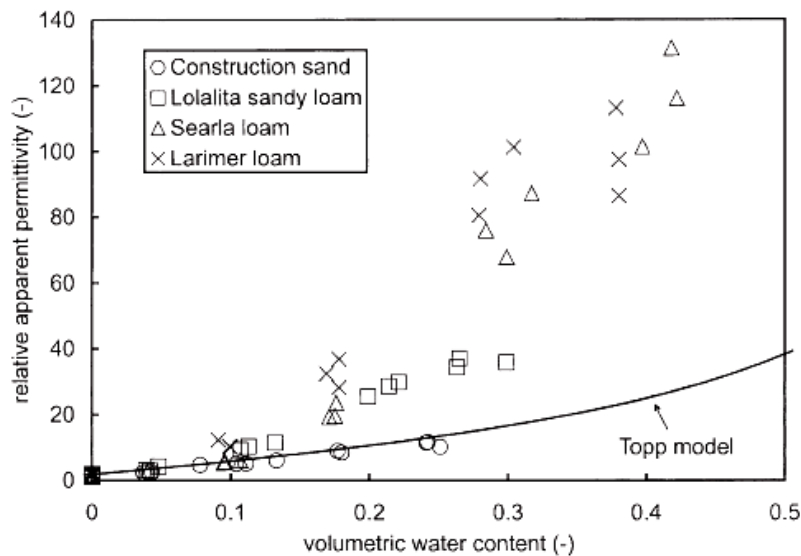


Figure 2.9: The calculated relative apparent permittivity [epsilon]_a as a function of volumetric water content for CS615 sensors in construction sand, Lolalita sandy loam, Searla loam, and Larimer Loam. (Kelleners et al. 2005)

2.3.5 Influence of Soil Density

An increase of soil density should lead to an increase of apparent dielectric constant. If the density increase is due to the increase of soil particles in a given control volume, because the value of soil particle dielectric constant is larger than one, the apparent dielectric constant should be increased; if the density increase is attributed to the increase of saturation rate, the volumetric water content is increased, so that an increment of apparent dielectric constant should also be observed.

Logsdon (1994) found that volumetric water content was linear related to bulk density:

$$\theta = -0.6709 + \frac{0.1288}{V_p} + 0.2690\rho_b \quad (\text{Equation 2.3})$$

where, V_p is the propagation velocity of signal in TDR waveguide, and ρ_b is the bulk density of soil.

Ledieu et al. (1986) also presented the volumetric water content as a linear function of bulk density:

$$\theta = 5.688t - 3.38\rho_b - 15.29 \quad (\text{Equation 2.4})$$

where, t is the travelling time of signal through wave guide, and ρ_b is the bulk density of soil.

A relationship between the apparent dielectric constant and the volumetric water for three series of samples, which were characterized by the dry densities of 1.4, 1.5, and 1.7 g/cm³ respectively, and compacted using the same soil type, is shown in Figure 2.10

(Pozzato et al., 2008). Topp's calibration was plotted as a reference in the figure. As can be seen, high dry density samples yield high apparent dielectric constant. Hence, compacted soils used in geotechnical applications usually have higher dry densities than those from Topp's database, so that Topp's equation might overestimate the volumetric water content for given K_a .

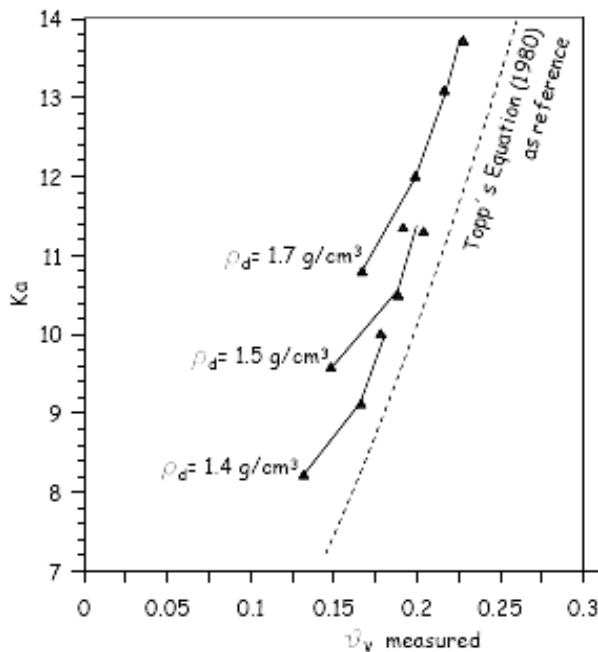


Figure 2.10: K_a versus vmc for the three different densities (Pozzato et al., 2008)

2.3.6 Influence of Temperature and freeze/thaw

Increases of apparent dielectric constant of four soils as the temperature increased were reported by Seyfried and Murdock (2004), shown in Figure 2.11. In this figure, sand showed the least sensitivity to temperature change, while “sheep creek” soil had its relative dielectric permittivity increased from 30 to 78 as temperature rise from 6°C to

46°C. This comparison not only showed the influence of temperature change, but also showed the effect of soil type on dielectric constant.

Similar phenomenon were also observed by Benson and Wang (2006), shown in Figure 2.12. The experiments used WCR CS-616 as the testing sensor, as will be discussed in this study, which is a type of low frequency TDR. The output of WCR is called reflecting period, which is the scaled traveling time of signals through wave guides. The testing temperature of Benson and Wang fell below the freezing point of water, namely 0°C. As can be seen, a significant decrease of reflecting period was observed as the temperature dropped to below 0°C.

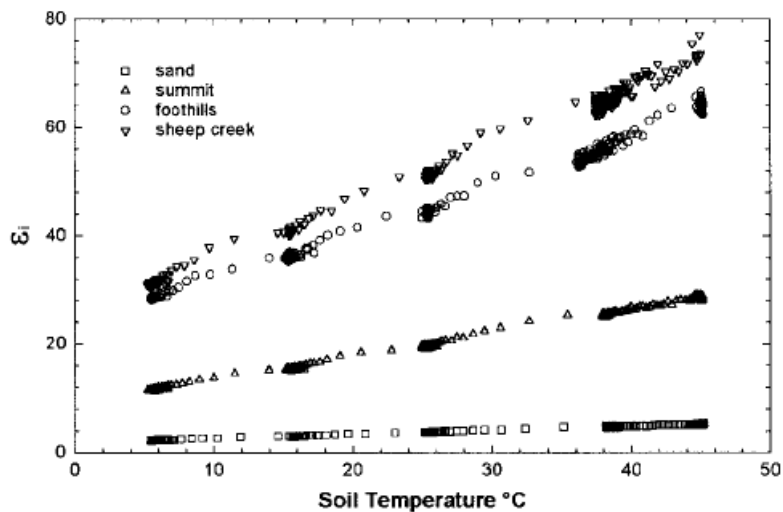


Figure 2.11: Effect of temperature on ϵ_i for the four soils measured at nearly saturated soil water contents (Seyfried and Murdock, 2004)

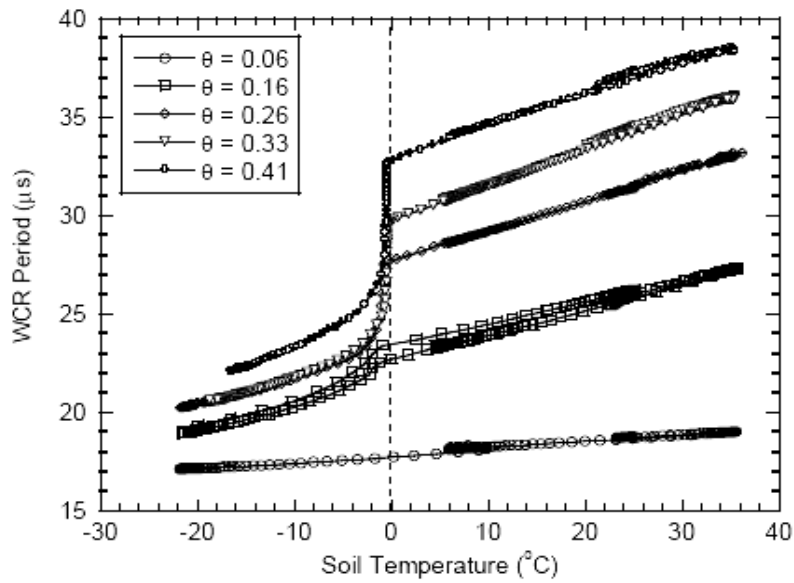


Figure 2.12: WCR Period as a Function of Soil Temperature for Soil A at Volumetric Water Contents (θ) of 0.06, 0.16, 0.26, 0.33, and 0.41. (Benson & Wang, 2006)

Chapter 3: Materials and Instrumentations

3.1 GEOTECHNICAL CLASSIFICATIONS OF SOIL

The soil used in this study is named RMA soil, which was obtained from a landfill cover system at Rocky Mountain Arsenal at Colorado. Ten 10-gallon buckets of soil, which had the original water content of 10-11%, were delivered to the laboratory in October, 2008. The particle-size distribution of the soil, shown in Figure 3.1, was determined following ASTM D 422-2007a. Sieve analysis was applied for particles larger than a #200 sieve (0.075mm). As can be seen, approximately 50% of the particles passed the #200 sieve. For finer portion, a hydrometer analysis was applied.

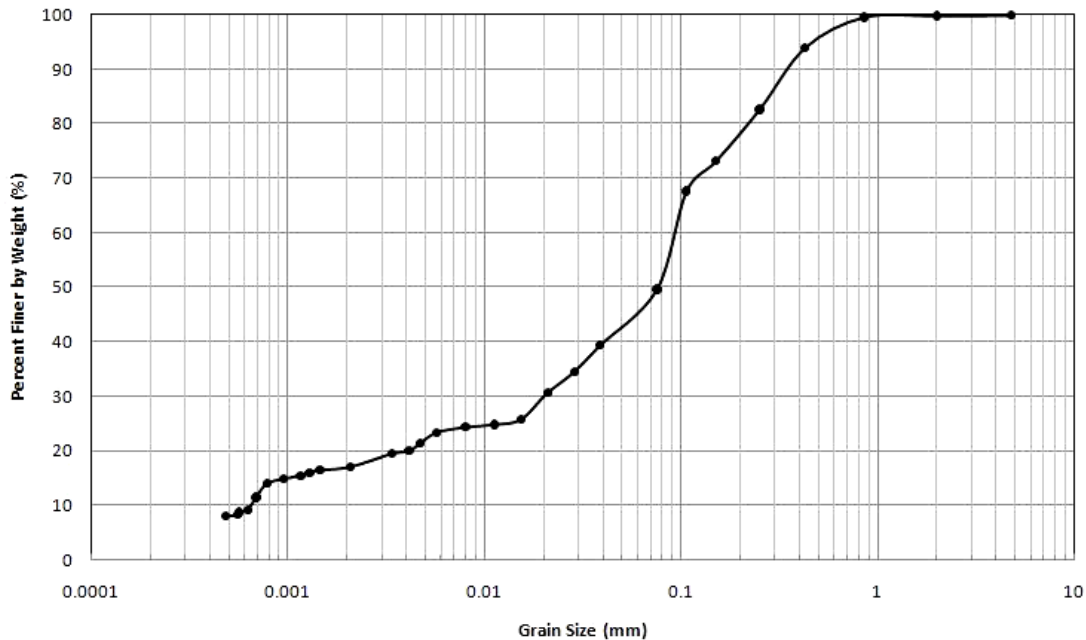


Figure 3.1: Particle-size distribution for New RMA soil (Thompson, personal communication)

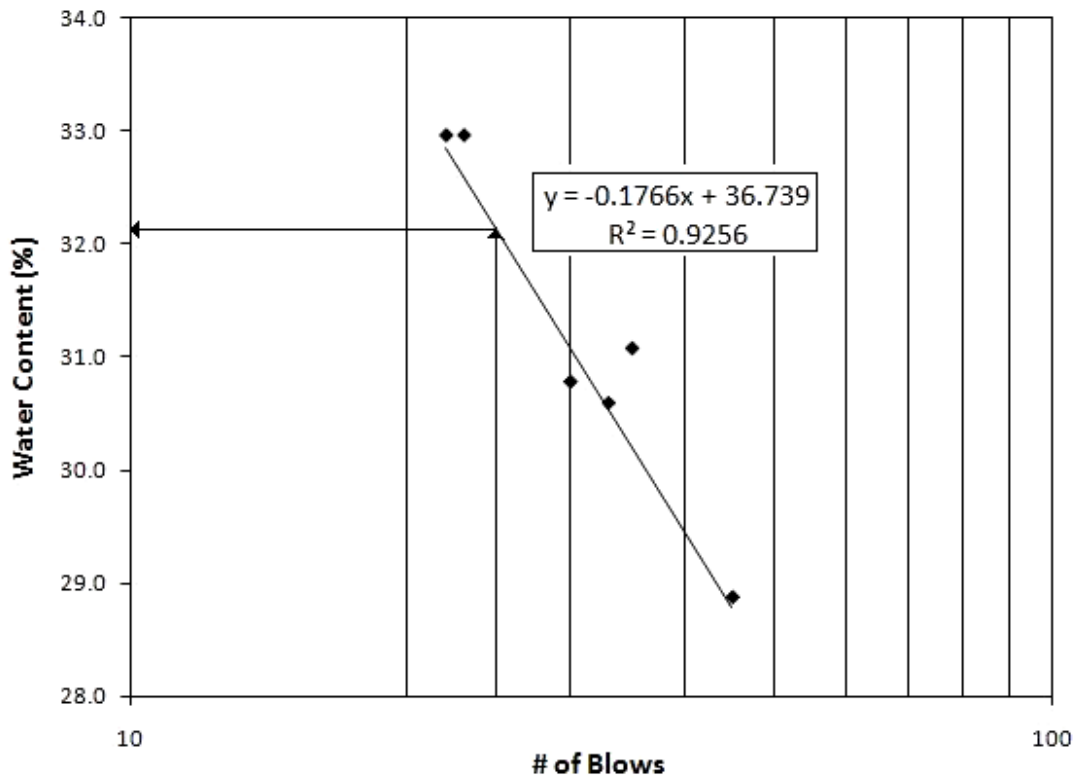


Figure 3.2: Liquid limit (Thompson, 2009, personal communication)

The specific gravity was determined to be 2.77 following procedures described in ASTM D 854 -2006a. The liquid and plastic limits were determined using methods presented in ASTM D 4318 -2005. The liquid limit (LL) was found to be 32%; Figure 3.2 shows the determination of liquid limit. The plastic limit (PL) of the soil was determined to be 12%, so the plastic index (PI) is 20% (PI=LL-PL). These geotechnical properties are summarized in Table 3.1. According to these values, the soil is classified as a Sandy Lean Clay (CL) based on Unified Soil Classification System (ASTM D2487).

Table 3.1: Geotechnical properties of RMA soil

Property	Value
D ₉₀	0.15mm
D ₅₀	0.075mm
D ₁₀	<0.0007mm
G _s	2.77
LL	32
PL	12
PI	20

3.2 COMPACTION CURVE

The compaction curve for RMA Soil was determined following procedures described in ASTM D698 with a standard proctor and a standard mold. The standard mold contains a base mold and a top cap; the inside diameter of the base mold is 10.16 cm, and the volume is 944 cm³; the top cap can be removed for extracting the specimen. A standard proctor, with mass of 2.58 kg and a drop height of 0.29 m were used to compact five layers with 23 blows per layer. The water content (w), which is the ratio of the mass of water to the mass of dry soil, was determined following ASTM D2216. The standard Proctor compaction curve is shown in Figure 3.3. The curve indicates that the optimum water content (w_{opt}) is approximately 14.3% and the maximum dry density ($\rho_{d,max}$) is 1.83 g/cm³, which is also called 100% compaction.

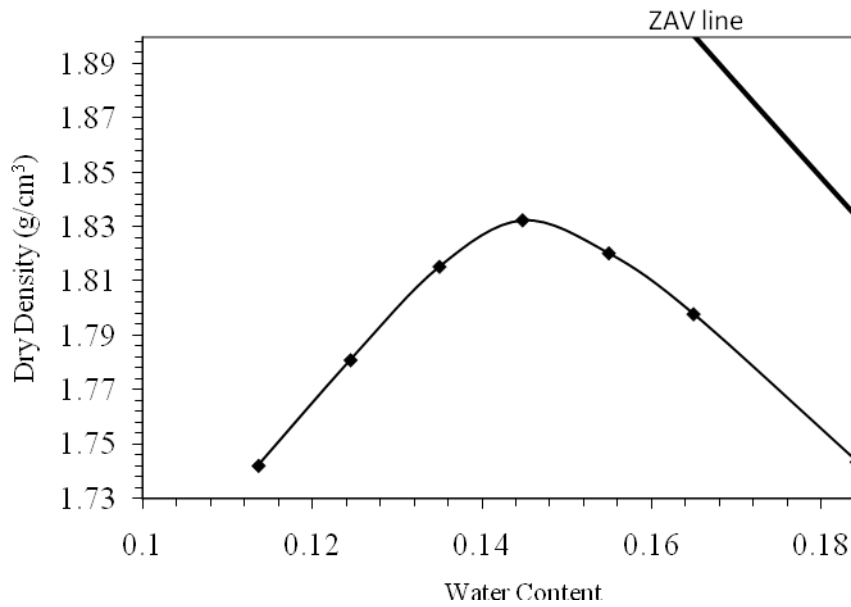


Figure 3.3: Standard Compaction Curve of RMA Soil

3.3 THE WCR REFLECTION CALIBRATION SYSTEM OVERVIEW

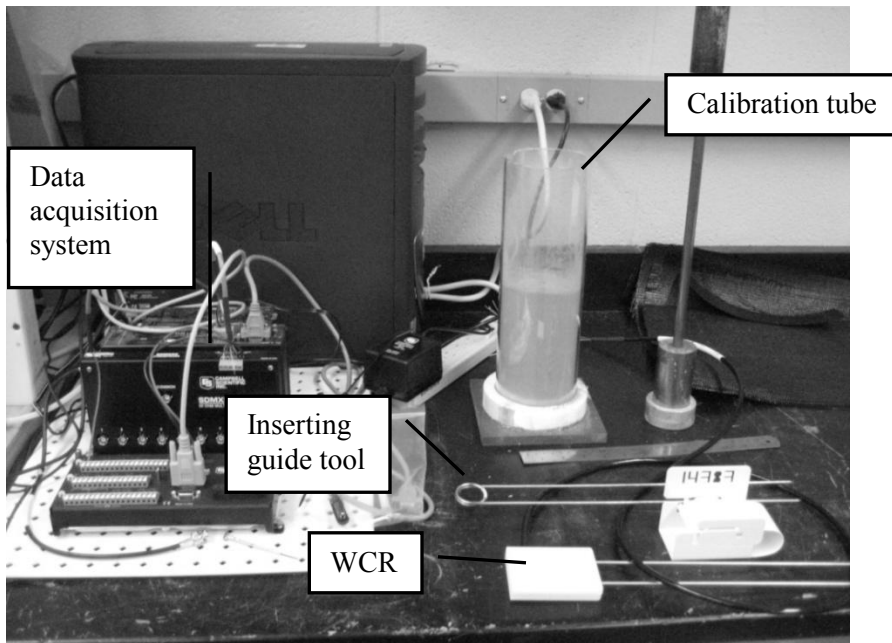


Figure 3.4: Apparatus Arrangement: (1) data acquisition system, (2) water content reflectometer, (3) inserting guide tool, and (4) calibration tube

As stated in Chapter 1, the goal of this study is to determine the response characteristics of WCR in RMA soil. In a basic calibrating system, RMA soil was prepared and contained in a calibration tube (Figure 3.4 and Figure 3.6), so that the water content (w) of soil was controlled; the reflectometer was inserted into soil specimen; signals from the reflectometer were then collected by a data acquisition system, and subsequently stored and visualized on a computer. These signals, named reflecting periods with units of mini second (ms), were referred to as the controlling parameters in calibration. Figure 3.4 shows the apparatus arrangement of this study: data acquisition system, water content reflectometer, inserting guide tool, and calibration tube.

As will be shown, the temperature fluctuation of the environment affected the signals obtained from WCR. Instrumentations that can control the specimen temperature were used to guarantee the calibration yielded steady outputs.

3.4 WATER CONTENT REFLECTOMETER: WCR CS-616

The water content reflectometer (WCR) CS-616 is manufactured by Campbell Sci., Logan, Utah. The WCR has two stainless steel rods, which are 30cm long, 0.32cm in diameter, with a spacing of 3.2cm, as shown on Figure 3.5. These rods serve as the path of wave propagation, where the wave propagation velocity depends on the dielectric permittivity of the surrounding soil. The rods is connected to a printed circuit inside the white box, from which, a black cable is connected. Inside the cable, there are four conductors, which are a power supplier, a signal trigger, and two output monitors.

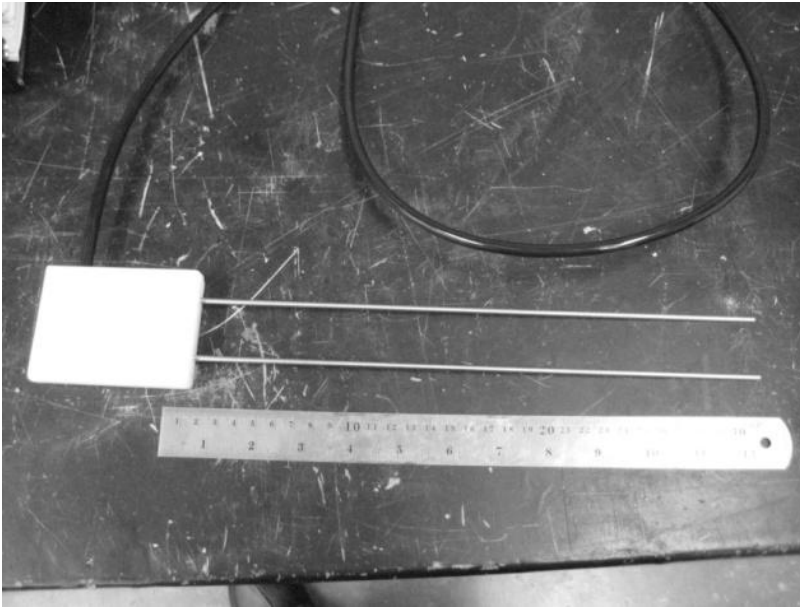


Figure 3.5: CS-616 Water Content Reflectometer

In operation, a wave front is generated and propagated along the rods by the WCR. Subsequently, the arrival of the reflection from the ends of the rods triggers a logic state change which initiates propagation of a new wave front. This process continues once the WCR is turned on. The time interval between two waves represents the wave propagation velocity. In soil, the time interval obtained is dependent on the water content, because water has a high dielectric permittivity, namely $\epsilon=80.1$, compared with soil (ϵ is around 4) and air ($\epsilon=1$) at room temperature.

TDRs are classified by their operating frequencies. Usually, the lower is the operating frequency the more affected by the soil type is the calibration of the TDR (Chandler et al. 2004). Compared to traditional TDR, which is with the operating frequency of approximately 1GHz, WCR is a type of low frequency TDR, whose

operating frequency is lower than 70MHz. For this reason, WCR response may be more soil specific. Nonetheless, the manufacturer provides only one calibration curve that is the same for the various types of soil.

The power supply of WCR is 12V DC, it is found that the response of WCR did not change while the power supply was adjusted from 11V-13.1V. In this study, a rechargeable 12V DC battery was applied as the power supply.

3.5 SOIL CONTAINERS

The soil container was constructed using a circular tube and a base, so that the soil can be extracted from tube and weighted. The dimensions of the circular tube were ID8.9 x H32 cm, as shown in Figure 3.6. The circular tube was made from transparent polycarbonate material, and the base was made from polyvinyl chloride (PVC) material. These materials are not electric conductors, so they will not affect the response of WCR. The soil container had a volume of 1.99l, while the theoretical sampling volume of WCR CS-616 is approximately 0.04l (Blonquist et al. 2005). The soil container should be large enough for satisfactorily calibrating. A top cap with the same diameter with the round tube was also constructed, allowing the compaction of top soil layer.

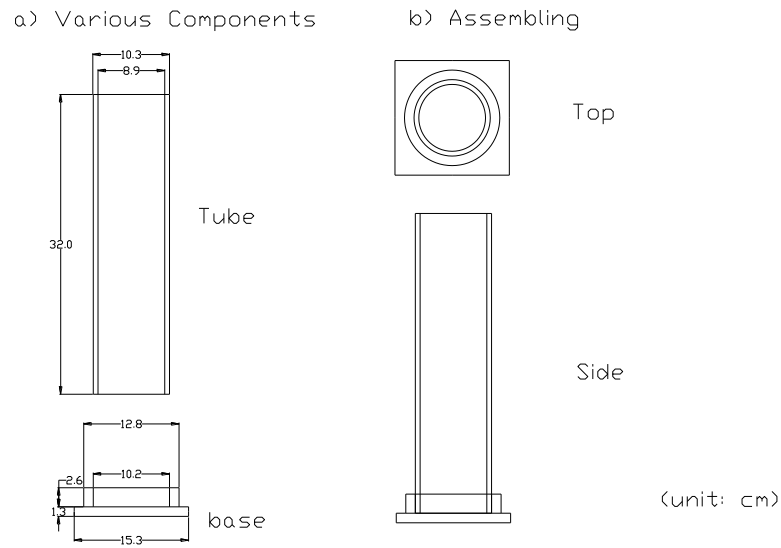


Figure 3.6: Calibration Tube: a) Various Components; b) Assembling

3.6 SOIL COMPACTION SYSTEM

In this study, the relative compaction of soil was used to classify the density of the specimen. As stated above, the 100% compaction of RMA soil using standard proctor method is 1.83 g/cm^3 . In the tests described in later chapters, lower relative compactions were chosen to investigate the impact of density to the response of WCR. Loose specimens were compacted to 75% relative compaction (1.37 g/cm^3), medium specimens were compacted to 80% relative compaction (1.46 g/cm^3), and dense specimens were compacted to 85% relative compaction (1.55 g/cm^3). A piston compactor was applied to adjust the compaction energy to achieve the different target relative compactions, shown in Figure 3.7.

The piston compactor has a piston with a diameter of 1cm. Compared to the cross-sectional area of the soil tube, the piston was considerably smaller. Unlike traditional

gravity compactor, which might make the upper portion of a layer denser than the lower portion, the whole layer of soil was observed to be compacted homogenously using the piston compactor.

In operation, the piston compactor was connected to a pressure meter, a regulator and a compressed air supply. The compaction energy was controlled by varying the pressure. With different compaction energy, different target relative compaction could be achieved.

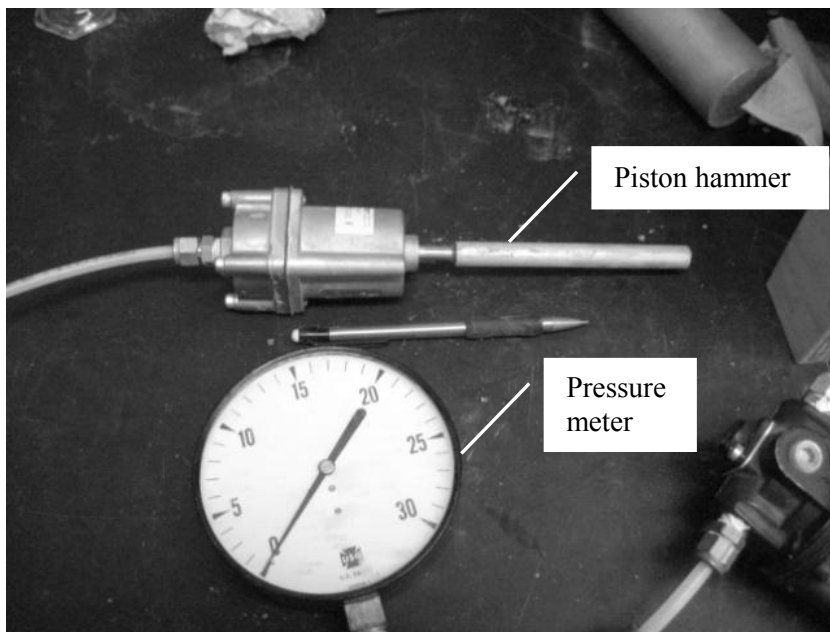


Figure 3.7: Air Piston Hammer

3.7 TEMPERATURE CONTROL SYSTEM

For the experiments conducted under room temperature, a plastic cooler was used to provide a constant temperature environment for the specimens, shown in Figure 3.8. As can be seen, three specimens were tested at the same time in the cooler. The cooler

had a 2 cm thick wall, which involved an air chamber between two plastic plates, blocking the heat dissipation. A hole was drilled to be the outlet for cables coming out on top the cooler. Around the rim of the hole, textile was used to wrap the cables, in order to fill the space between the rim and cables. A temperature sensor was also installed inside the cooler, so that the temperature inside could be monitored continuously.

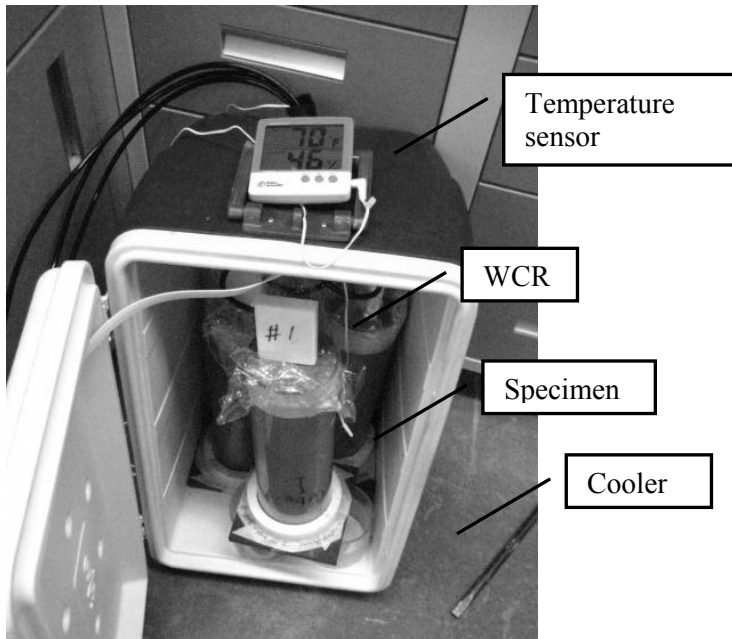


Figure 3.8: Experiment Environment

Test results obtained with a WCR under room temperature in 24 hours (2:00pm-2:00pm) without any temperature confinement are shown in Figure 3.9. As can be seen, the WCR responses fluctuated as the room temperature changed periodically. In comparison, another record is shown in Figure 3.10. This test was conducted inside the cooler in late December, 2008. Though the winter air conditioning system made the room temperature fluctuated sharply, the WCR responses did not show significant change.

Instead, it converged to a constant value at the end of the test. This comparison between Figure 3.9 and Figure 3.10 shows the cooler isolated the experiments from room temperature changes effectively and satisfactorily.

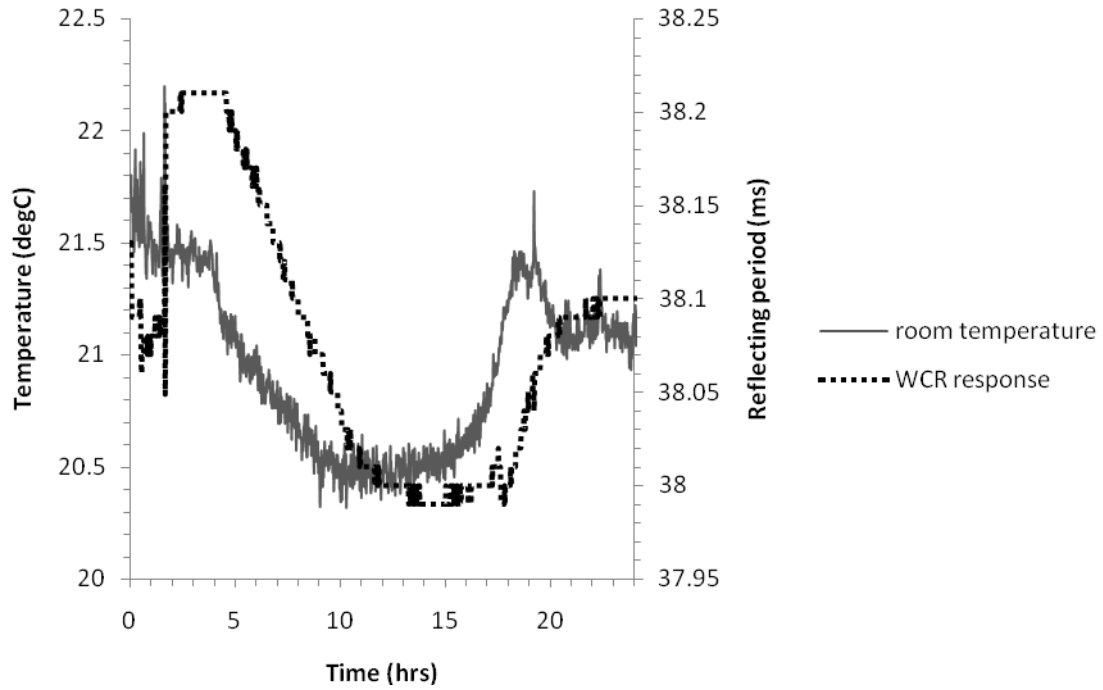


Figure 3.9: Room temperature and WCR response tested in room

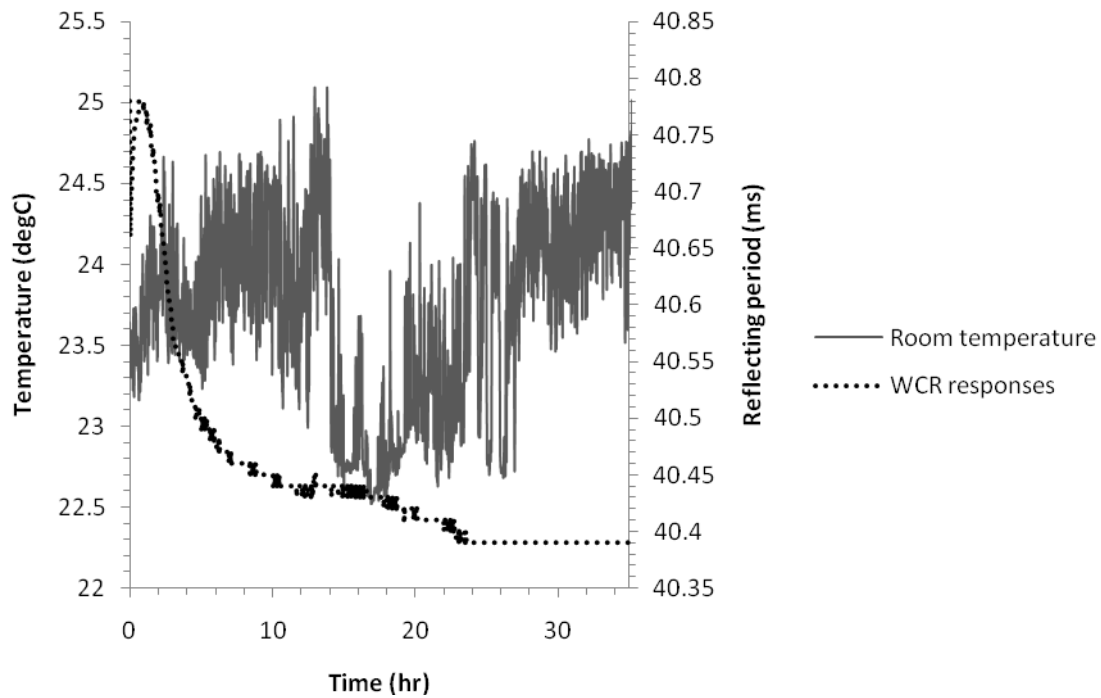


Figure 3.10: Room temperature records and WCR responses in a cooler

For testing the WCR responses in a wide range of temperature, a temperature control system that could provide a testing environment ranging from -20°C to 40°C was constructed. This system contained three main components: a freezer, heating elements and a temperature controller. Figure 3.11 shows the wiring diagram of the temperature control system.

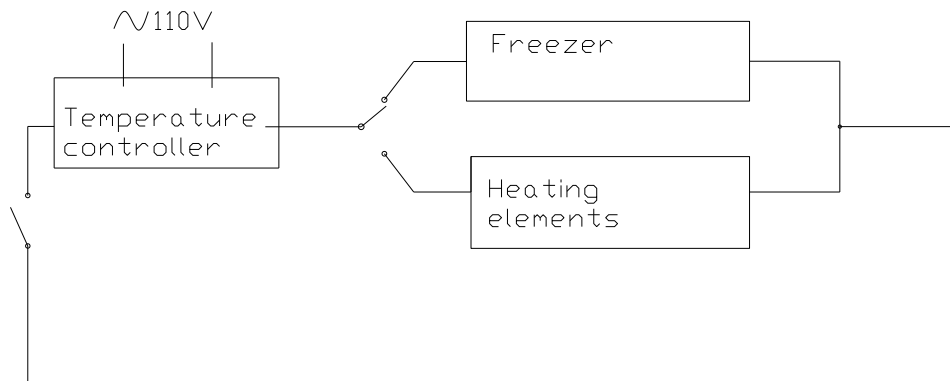


Figure 3.11: Circuit of temperature control system

Temperature controller worked as the enabler in this system using RANCO[®] ETC, shown in Figure 3.12. It provided on/off control for heating or cooling apparatus. A temperature sensor was connected to the controller, and the reading from the sensor would be displaced on the LCD screen.

The high testing temperature was achieved using HotWatt[®] heating elements, shown in Figure 3.13. These electric heaters had the normal operating voltages of 50V. For the sake of safety and maneuverability, in this study an 11V DC power supply was used for the heating elements instead of 50V. To compensate the power loss due to reduced voltage, four heating elements were paralleled inside the testing chamber.

The low temperature testing environment was provided using a GE[®] compact chest freezer, shown in Figure 3.14. The freezer could reach temperature as low as -21°C, which was lower than the required testing range in this study. The freezer was not only the cooling instrumentation but also the testing chamber for wide temperature range testing.



Figure 3.12: Temperature controller

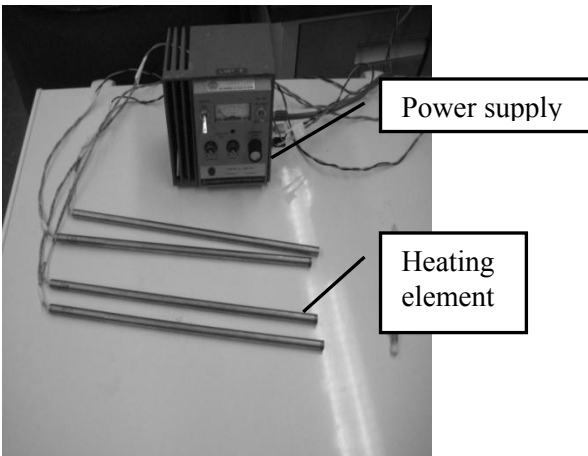


Figure 3.13: Heating elements and electric power supply



(a)



(b)

Figure 3.14: Freezer: (a) outside; (b) inside

In operation, soil specimens were placed inside the freezer; heating elements were hanged in the top portion of the inside space of the freezer. For heating process (when the target temperature was higher than room temperature), the temperature controller was in series with the heating elements; the circuit was enabled as long as the current temperature inside the freezer was lower than the target temperature; once the current temperature reach the target temperature, the temperature controller would turn off the heating elements. For cooling process (when the target temperature was lower than room temperature), the temperature controller was in series with the freezer; the freezer would be keep working till the current temperature inside reach the target temperature. The logic of the temperature control system is illustrated as flowcharts in Figure 3.15.

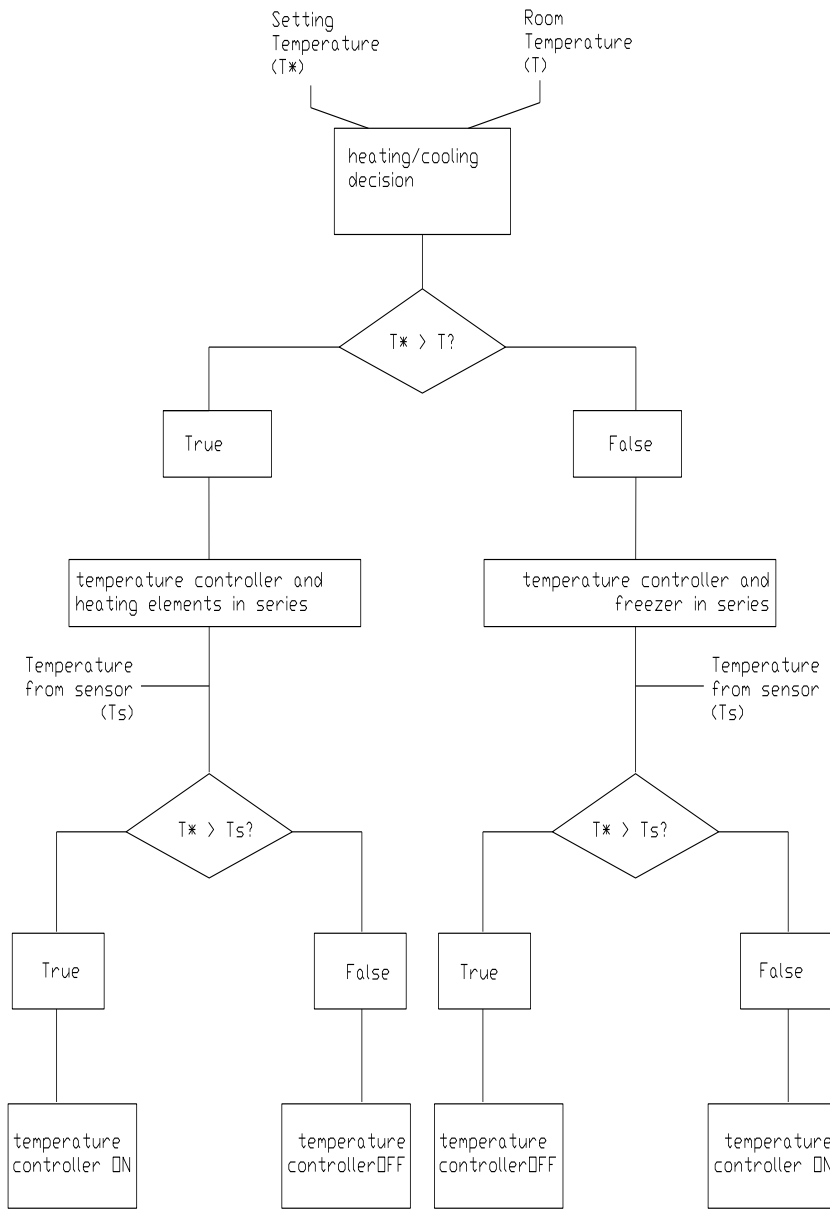


Figure 3.15: Flowcharts of temperature control system

3.8 DATA ACQUISITION SYSTEM

The data acquisition system used in this study was the CR1000[®] data logger, developed by Campbell Sci., of Logan, UT, shown in Figure 3.17. The data logger had 16

single-ended\8 differential-ended inputs meaning that 16 WCRs could be measured at the same time. Once the program was sent to and compiled by the data logger, the WCR testing would be enabled and continued till testing program was re-sent or the storage was full. Readings from WCRs were stored in the data logger, and could be instantly visualized on a PC.

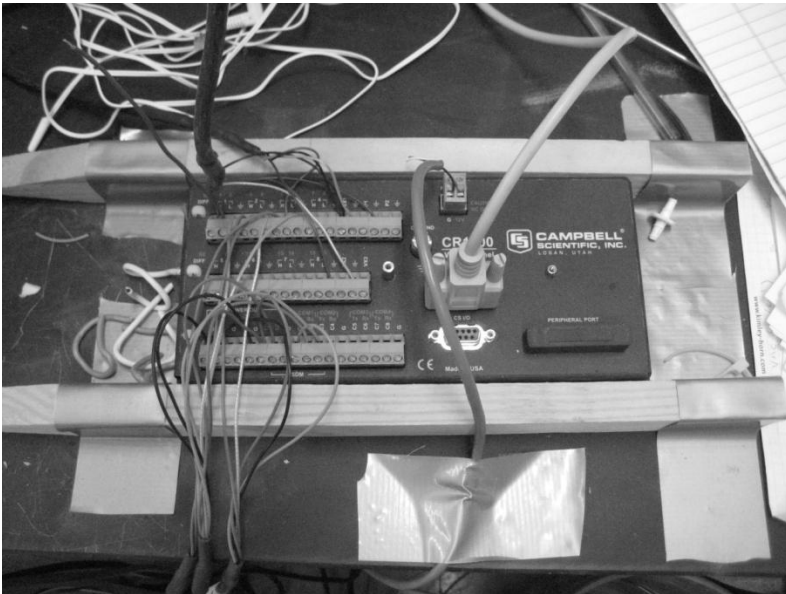


Figure 3.17: Data logger CR1000

Chapter 4: Experimental Procedures

4.1 OVERVIEW

Two important goals of the experiments were to examine the responses of WCR for different soil dry densities and to investigate the temperature effect on WCR testing. In this study, two series of experiments which respectively focused on dry density effects and temperature effects were conducted. For the series focused on dry density effects, three sets of tests with different relative compactions (75%, 80%, and 85%) were conducted; in each set, specimens of different water contents were prepared. For the series focused on temperature effects, six tests of different water contents were conducted. This chapter presents the methodologies and assumptions of the two series of experiments, along with the testing procedures. Though the testing results will be presented and discussed in Chapter 5 and 6, the testing scope and parameter selection is presented in this chapter.

4.2 TESTS FOR CALIBRATING WCR WITH DIFFERENT SOIL RELATIVE COMPACTIONS

4.2.1 Basic philosophy and assumptions

As presented in section 3.4, the reflecting period (T) represents the time for a wave propagating back and forth through the circuit and steel rods of WCR. The propagating time is determined as a function both the delay of the circuit and the dielectric constant of the material around the rods (Kelleners et al. 2005):

$$T = 2\left(t_d + \frac{2L\sqrt{K_d}}{c}\right) \quad (\text{Equation 4.1})$$

where t_d is the time delay through the circuit and cables, L is the length of rods, K_a is the apparent dielectric permittivity of the soil, and c is the velocity of light in free space.

t_d might be determined by the circuit components, for a given wiring condition, t_d was assumed to remain a constant value.

K_a , the apparent dielectric permittivity of the soil, may be obtained using a three-phase model (Zakri et al. 1998):

$$K_a = (\varphi_a \varepsilon_a^\alpha + \varphi_s \varepsilon_s^\alpha + \varphi_w \varepsilon_w^\alpha)^{1/\alpha} \quad (-1 < \alpha < 0, 0 < \alpha < 1)$$

(Equation 4.2)

where φ_a , φ_s , and φ_w are the volumetric portions of air, soil particles and water respectively; ε_a , ε_s and ε_w are the dielectric permittivity of air, soil particles and water respectively. Because ε_w is believed to be usually 10 to 15 times larger than ε_s , and 80 times larger ε_a , the value of φ_w , namely the volumetric water content, is the determinant factor in this equation. In addition, since the porosity (n) of a soil specimen decreases as the relative compaction of the soil specimen increases, φ_s increases and φ_a decreases with increasing soil dry density (γ_d). As a result, K_a should increase with increasing γ_d , yielding a higher reflecting time (T).

4.2.2 Testing scope and testing procedures

To validate the philosophy and assumptions discussed in previous section, three sets of soil specimens were prepared and tested, each with a different relative target compaction of 75%, 80% and 85%. It should be noted that the 100% relative compaction

corresponds to 1.832kg/m^3 . However, because of the difficulties for acquiring constant dry density while the moisture content is changed, our specimen series are not of exact dry density as stated above. The dry densities of 75% representative group are within $1.41\pm 0.03\text{ kg/m}^3$; the dry densities of 80% representative group are within $1.48\pm 0.03\text{kg/m}^3$; the dry densities of 85% representative group are within $1.56\pm 0.03\text{kg/m}^3$. For each relative compaction, the volumetric water content of the specimens was varied in order to define the calibration curve for moisture ranging from 0% to 38%.

The first step of testing procedure involved preparing and cleaning the soil containers. The dimensions and details of the containers were mentioned in section 3.5. Each component was weighed individually; the bottom outer rim of the circular tube was coated with silica gel; subsequently, the circular tube was placed on top of the base.

The second step was to moisten soil to the target moisture content and compact it into the container. The characteristics of the soil were stated in section 3.1 and 3.2. Initially, the soil was dried and smashed into small particles; subsequently, the dry soil was placed on a plate and the amount of water corresponding to the target θ was slowly added to soil while mixing it. Before compacting soil into the container, a target weight per lift was calculated according to the relative compaction and target water content. The moistened soil was compacted in five lifts into the container using an air piston compactor, as described in section 3.6, to knead the soil. The number of blows per lift and the air pressure used during compaction varied according to required relative compaction. A gauge was used to guarantee each lift reach the target density.

The third step was to seal the soil specimen and insert the WCR sensor. The method of sealing varied according to the type of specimens. Two types of specimens were prepared for quantifying the responses of WCR: TYPE I Pre-wetted Specimen, and TYPE II Post-wetted Specimen. In pre-wetted specimens the soil sample was mixed using a predetermined amount of water, and was isolated from outside air and water after mixing, so the water content of the specimen was supposed not to change during testing; while in post-wetted specimens the soil sample was prepared using a relatively low water content, but a certain amount of water was subsequently placed on top of it, so water would infiltrate into the specimen in order to achieve the target water content. Post-wetted specimens were used especially to acquire readings when soil was at a high degree of saturation.

For a TYPE I specimen, after the moistening and compaction discussed above, the WCR insert-guide tool was inserted in the center of the specimen. The guiding tool had the same rod-spacing, rod diameters, and rod lengths as the WCR. It drilled paths for the installation of WCR. A view of a TYPE I specimen is shown in Figure 4.1.

For a TYPE II specimen, after mixing and compacting, two guiding paths were also driven in the specimen. Next, a top cap was installed above the tube. Certain amount of water is subsequently poured into the top cap. Water then slowly infiltrated into the soil making the moisture content increase. The set-up of a TYPE II specimen is shown in Figure 4.2.

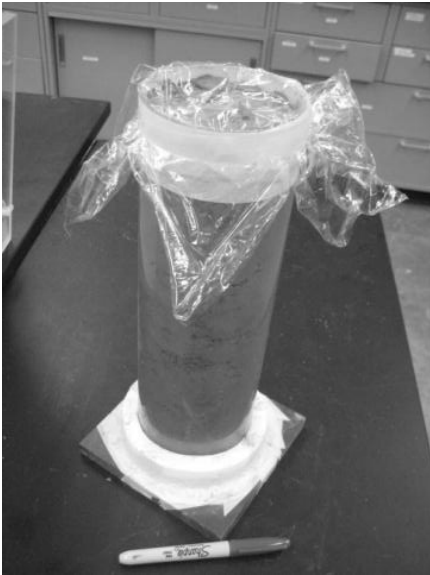


Figure 4.1: A Prepared Pre-wetted Specimen

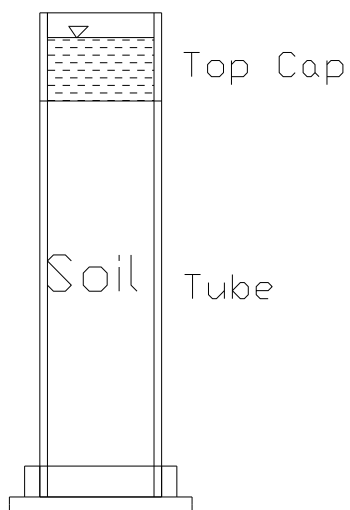


Figure 4.2: A scheme of a post-wetted specimen

After finishing preparation, the WCR probe was inserted following the paths drilled by the guiding tool, as shown in Figure 4.3 and Figure 4.4. The top of the tube was then wrapped with plastic membrane in order to isolate the soil from atmosphere.

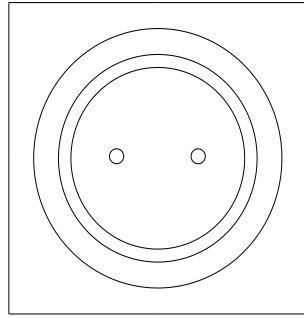


Figure 4.3: The two-prong path from the top of the specimen

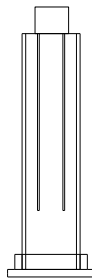


Figure 4.4: Reflectometer in tube

The fourth step was to enable the WCR testing program, and take readings to track the response continuously. After specimen preparation, the specimens were placed inside a cooler in order to get rid of the impact of temperature change in lab. The details and effects of the cooler were described in section 3.7. The temperature inside the cooler was also continuous monitored. Although the soil was mixed and moistened carefully, the moisture distribution within the soil specimen might not be homogeneous, thus, the WCR response might not be consistent with the water content initially. For this reason, a period of waiting was needed for the redistribution of water inside the specimen finishing; during the time the response from WCR was continuously recorded, till the response

converged to a constant value. Once the reading converged to a constant value, it could be assumed that the movement of moisture inside was ceased, reaching an equilibrium stage. At this stage, moisture was considered distributed homogeneously in the specimen, meaning that any portion of the specimen was of the same water content. As a result, the response from WCR could represent the water content of the whole specimen. In this study, a 40-hour waiting time was adopted before selecting the representative WCR response. The selection philosophy and the determination of waiting time will be presented in Chapter 5.

Eventually, the gravimetric water content of the soil specimen was measured, using the oven drying method presented in section 2.2.1. The gravimetric water content was subsequently converted to volumetric water content.

4.3 TESTS FOR CALIBRATING WCR IN VARIED TEMPERATURES

The temperature effect of WCR response was investigated using temperature ranging from -20°C to 40°C . The relative compaction of specimens tested in this series was 80%, namely $1.47\text{kg}/\text{m}^3$. The volumetric water contents of the specimens were varied from 2.8% to 33%. In this study, specimens were first heated from room temperature (approximate 21°C) to 40°C , and they were then cooled down gradually to -20°C . In order for WCR measurements in this temperature scope to be consistent, it was assumed that a given specimen at a given temperature was corresponded to only one WCR response value, ignoring the possible hysteresis effect in heating-cooling process (Benson and Wang, 2006).

The approaches used for container preparation, soil moistening, soil compaction, specimen sealing, and sensor installation were the same as from those presented in section 4.2. After preparation, the specimens were placed into the temperature control system. The temperature control system could maintain the inside of the chamber at a target temperature. The arrangement, components, and operations of the temperature control system were described in section 3.7. The arrangement inside the temperature control system is shown in Figure 4.5. In this study, three specimens were usually tested at one time in order to step up the rate of progress.

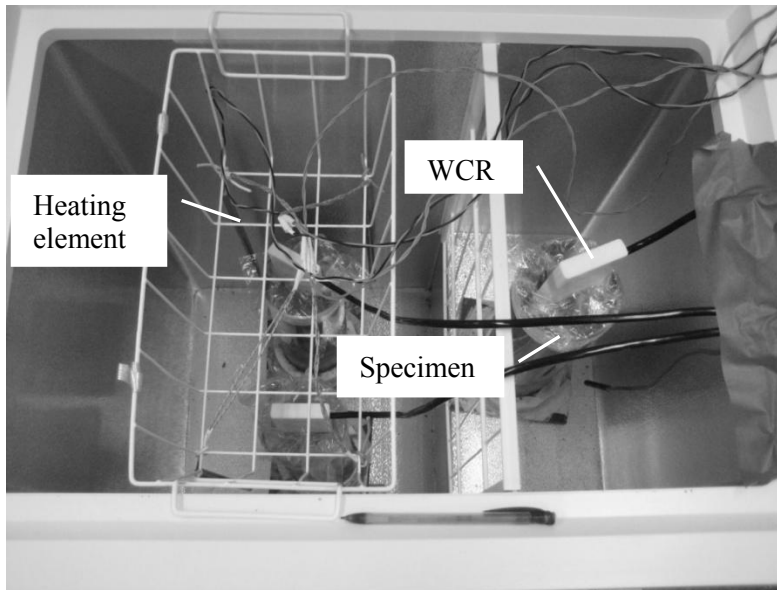


Figure 4.5: The arrangement inside temperature control system

Tests were conducted starting at the initial target temperature of 40°C. Further, the target temperature was lowered every time by 5°C to obtain the next WCR measurement, and consequently reach the lowest target temperature, namely -20°C. The testing span between two temperature changes was 24 hours because soil specimens need

a certain period to reach thermal equilibrium. However, in the first temperature change, namely from room temperature to 40°C, the specimens were tested for 40 hours, because for the new prepared specimen require time not only for thermal equilibrium but also soil moisture equilibrium.

Chapter 5: Effects of Relative compaction on WCR Calibration Curves

5.1 OVERVIEW AND A TYPICAL RESULT

The experiments conducted to examine the WCR response in RMA soils with different relative compactions included two types of specimens; each type has identical preparation method, as stated in Chapter 4. This chapter presents the testing setup, results, and explanations of results, while data interpretation will be presented in Chapter 7. The specimens for testing were prepared using relative compaction value of 75%, 80% and 85%. The setup of experiments is shown in Table 5.1.

Table 5.1: The setup of experiments

Temperature (°C)	Voltage of power supply (V)	Interval between measurements (sec)	Testing duration (hr)
21.5	12.9	60	48

Figure 5.1 shows a typical WCR response using RMA soil over time. As can be seen, the readings fluctuated at the initial stage. This fluctuation may be attributed to the redistribution of moisture within soil specimens. After a period of time, usually approximately 40 hours, the WCR response converged to a certain value. As was discussed in Chapter 4, the water transportation was assumed to be stopped at this stage, which named equilibrium stage. In this study, a testing duration was 48 hours was adopted, as shown in Table 5.1, for the sake of waiting for equilibrium. The WCR

responses at the end of experiments were selected as the representative reflecting periods corresponding to the water content of specimens.

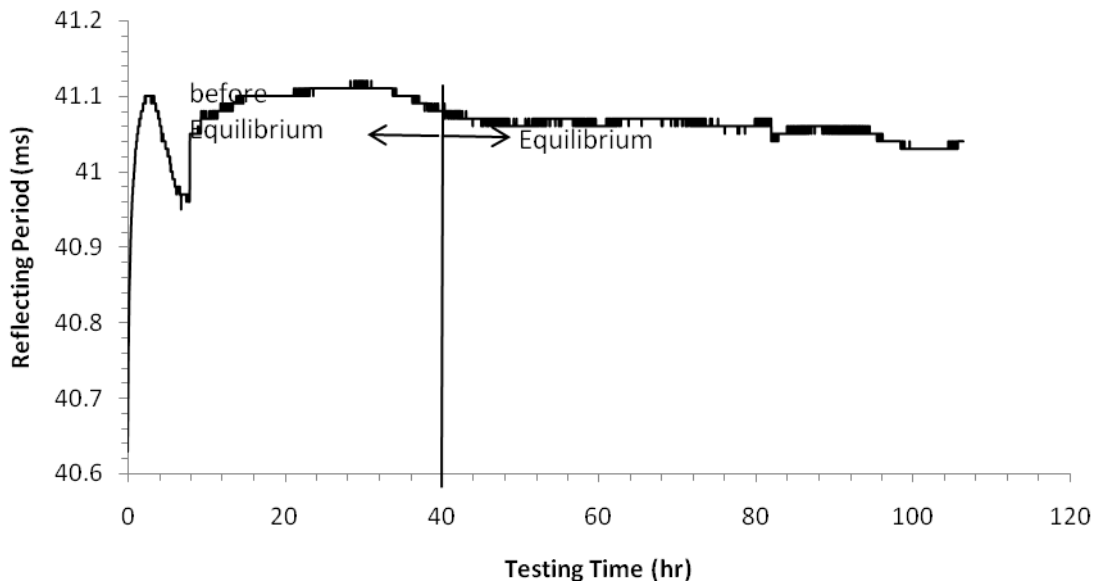


Figure 5.1: Typical readings from 0 to 110 hrs in RMA soil

Figure 5.2 and Figure 5.3 show the WCR responses in dry air and in water over time. Unlike the test in soil, the readings in these two tests almost did not change from the beginning to the end (in dry air, 14.96ms; in water, 43.67ms). According to the assumptions of equilibrium and moisture redistribution, the reason for the phenomenon is, in either water or dry air, there were not processes of water transportation as within soil specimens. The two tests shown in Figure 5.2 and Figure 5.3 were conducted in October 2008; another two tests in dry air and pure water were conducted in March 2009, and they yielded same reflecting periods as those conducted four months before, indicating that the working quality of WCR sensors was likely stable.

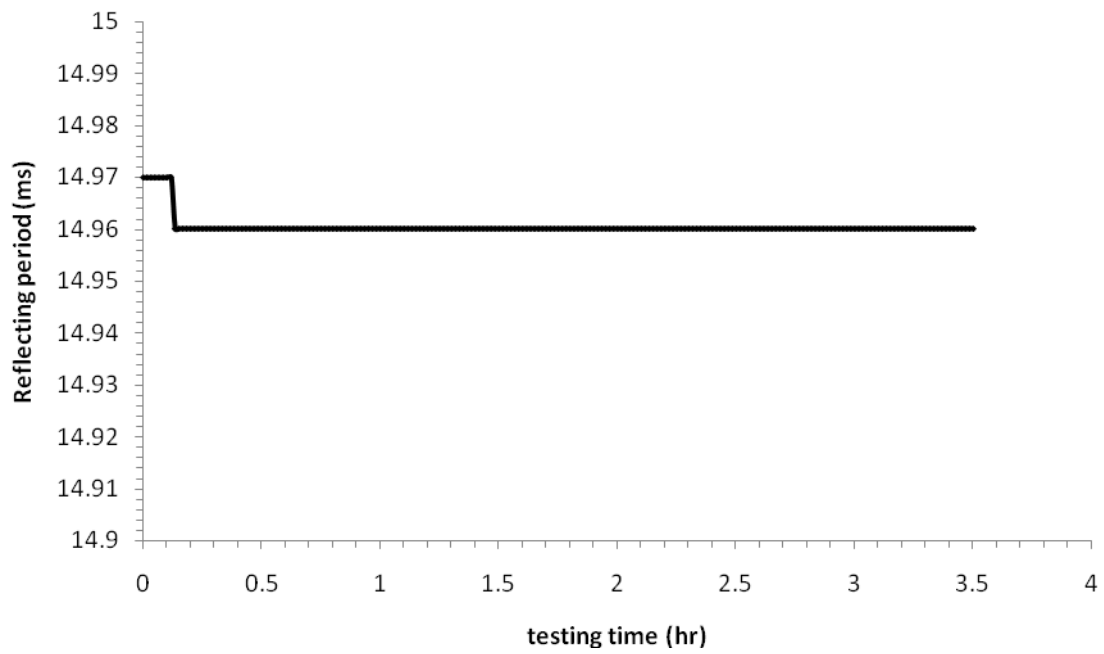


Figure 5.2: WCR responses in dry air

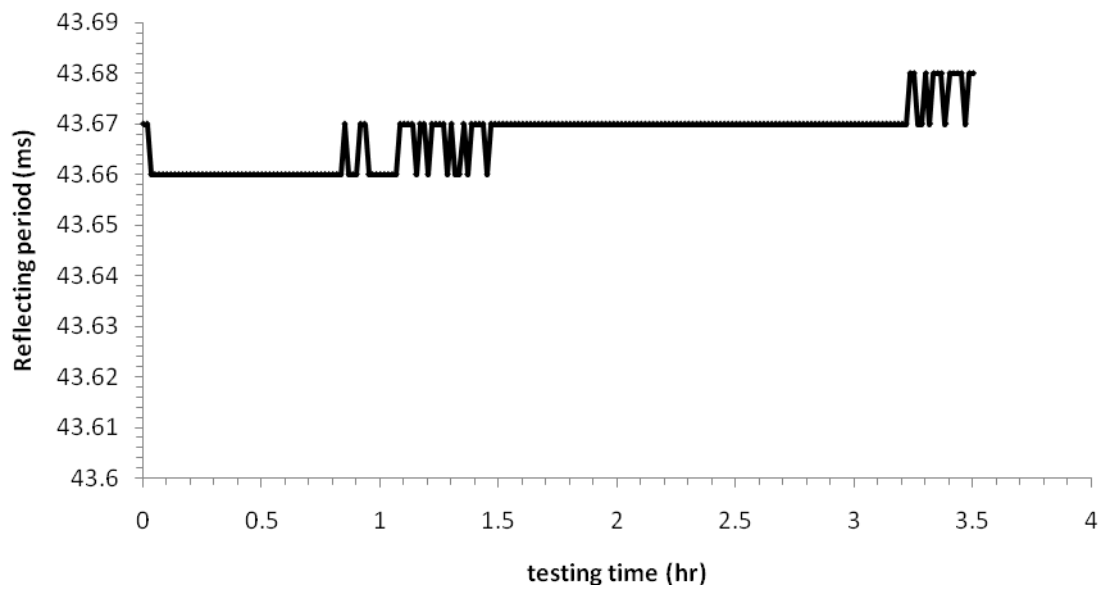


Figure 5.3: WCR responses in water

5.2 SUMMARY OF WCR CALIBRATION RESULTS

Figure 5.4 shows a specimen after a 48-hour test, on which imposing flow method was applied. As can be seen, the specimen expanded specifically, 7.5mm vertical swelling was measured for an original specimen length of 320mm. The expansive characteristic of soil made the preparation and control for reaching target dry densities challenging.



Figure 5.4: A specimen after testing

The dry density and degree of saturation distribution of all specimens is presented in Figure 5.5. As shown in the figure, the overall range of degree of saturation is wide, namely from 0.15 to 0.85. However, the 75% set includes degree of saturation only up to 0.63, because the mixed soil was so compressible that it was impossible to prepare samples without obvious cracks or gaps at higher degree of saturation. Also, for the 85% set, specimens were prepared for degree of saturation only over 0.40. This is because the

soil was considerably stiff when dry. To reach the target relative compaction at lower degree of saturation, a more powerful kneading tool was required.

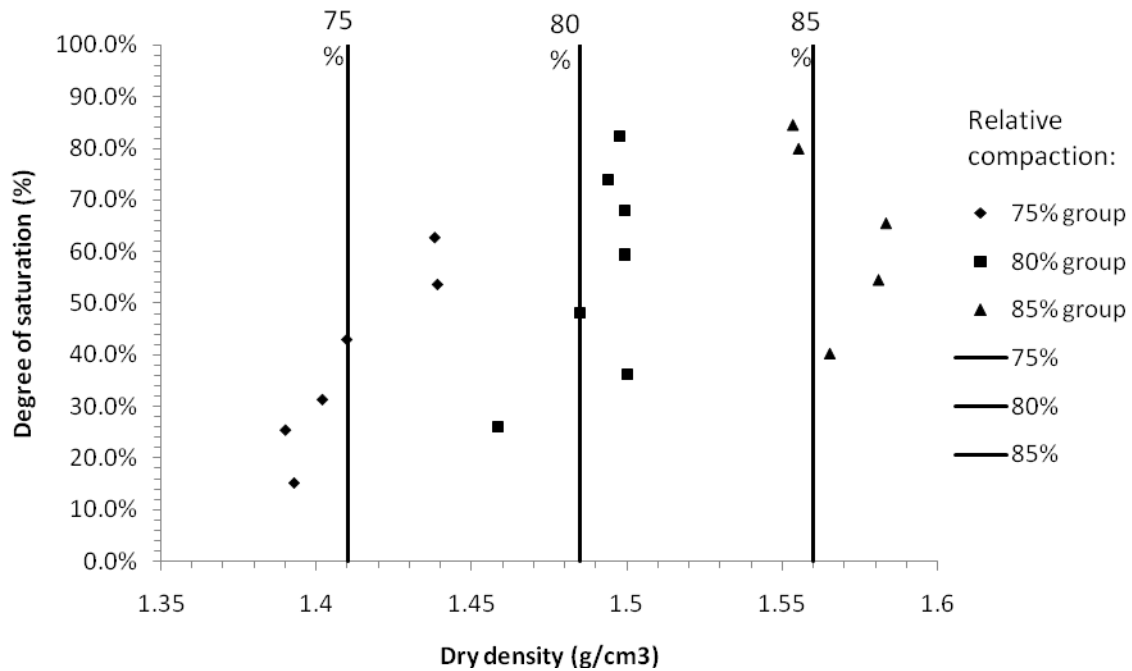


Figure 5.5: Actual dry density and volumetric water content distribution in the three test sets

The results of all tests for three different target relative compactions (75%, 80%, and 85%) are presented in Table 5.2, Table 5.3, and Table 5.4. As shown in tables, the responses in dry air and in water were found to be the lower and upper bounds of readings.

Table 5.2: Data of 75% set

dry density: γ_d (g/cm ³)	Volumetric moisture content: vmc (g/cm ³)	Degree of saturation: Sr	Reflecting period (ms)
---	---	-----------------------------	---------------------------

DRY AIR	0	0	14.96
1.392769462	0.075342	0.151534	21.30332
1.389986304	0.126468	0.253851	25.96618
1.401835005	0.154533	0.312869	29.02809
1.409677214	0.210684	0.429012	32.97726
1.438832925	0.257397	0.535613	35.8842
1.437972086	0.301164	0.626282	36.325
WATER	1	1	43.67

Table 5.3: Data of 80% set

dry density: γ_d (g/cm ³)	Volumetric moisture content: vmc (g/cm ³)	Degree of Saturation: Sr	Reflecting period (ms)
DRY AIR	0	0	14.96
1.45848962	0.123596	0.261043	26.47146
1.500188191	0.166362	0.362906	31.42021
1.485026605	0.222754	0.480188	34.93093
1.499420965	0.272347	0.593746	37.61966
1.499474548	0.311487	0.679105	39.22456
1.494172396	0.340408	0.739073	39.36164
1.497842027	0.37759	0.822166	39.50763
WATER	1	1	43.67

Table 5.5: Data of 85% set

dry density: γ_d (g/cm ³)	Volumetric moisture content: vmc (g/cm ³)	Degree of Saturation: Sr	Reflecting period (ms)
DRY AIR	0	0	14.96

1.565192495	0.174612	0.401455	33.52
1.581013482	0.23366	0.54436	36.39
1.58347503	0.28023	0.654212	38.35
1.555065603	0.350267	0.798593	40.5
1.553198408	0.370962	0.844479	41.06
WATER	1	1	43.67

The experimental data is summarized in Figure 5.6. The figure shows that the reflecting period from WCR is a function of the volumetric water content of soil for each relative compaction. The reflecting period increases with increasing volumetric water content. However, the increasing rate shows an opposite trend: in high water content portion the slope of reflecting period trend is steeper than that in low water content portion. Take the 80% set for example, the reflecting period increases by 2 ms as the volumetric water content increases from 0.27 to 0.37; however, the rise is 6 ms as the volumetric water content increases from 0.17 to 0.27.

Additionally, for given volumetric water content, reflecting period increases with increasing relative compaction (increasing dry density). Note that the dry density of soil is a measurement of the quantity of soil particles in unit space of moistened soil. Nonetheless, Figure 5.6 also shows that the differences of reflecting periods between different relative compactions were likely constant at all volumetric water contents. The value of the difference is approximately 0.9-1.0 ms.

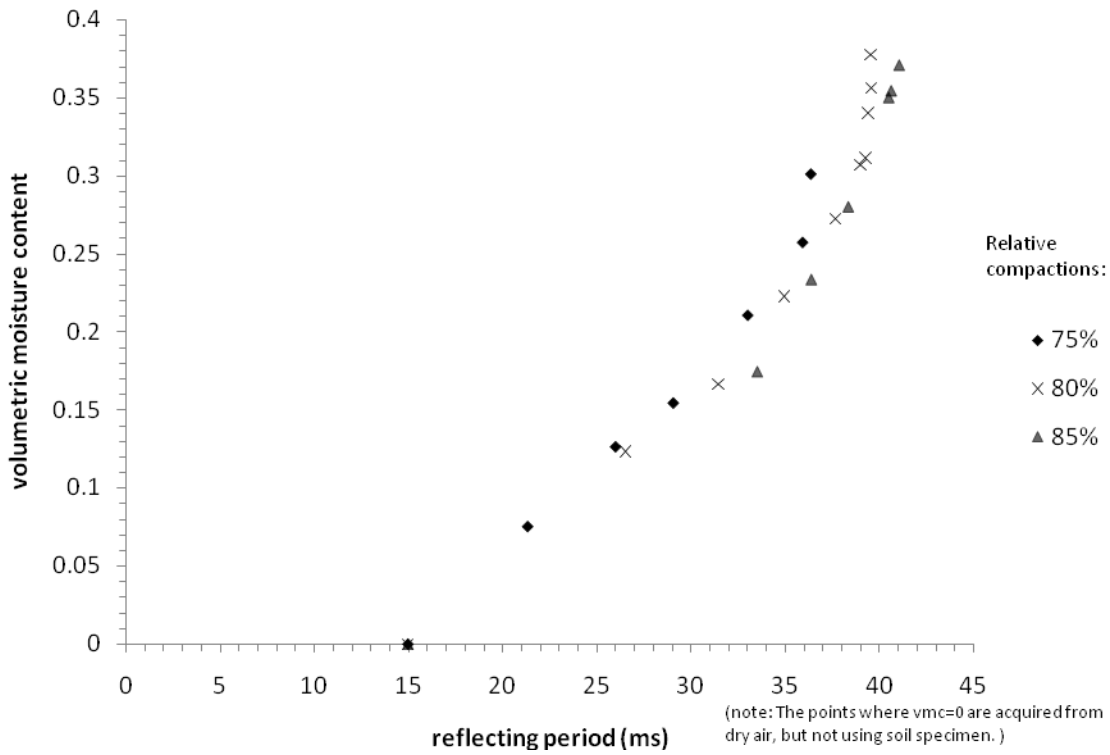


Figure 5.6: The volumetric water content and time relations at different relative compactions

The testing results indicate that both water and soil particles affect the dielectric properties of soil. As stated in Chapter 4, the reflecting period of WCR was governed by the apparent dielectric constant of soil, and it was assumed that this relation could be resolved by a three-phase model:

$$Ka = (\varphi_a \varepsilon_a^\alpha + \varphi_s \varepsilon_s^\alpha + \varphi_w \varepsilon_w^\alpha)^{1/\alpha} \quad (-1 < \alpha < 0, 0 < \alpha < 1)$$

(Equation 5.1)

where φ_a , φ_s , and φ_w are the volumetric portions of air, soil particles and water respectively; ε_a , ε_s and ε_w are the dielectric permittivity of air, soil particles and water

respectively. Because ε_a is 1 in free space, the term $\varphi_a \varepsilon_a^\alpha$ can be neglected. As a result, the model could be reformed as follows:

$$Ka = (\varphi_s \varepsilon_s^\alpha + \varphi_w \varepsilon_w^\alpha)^{1/\alpha} \quad (-1 < \alpha < 0, 0 < \alpha < 1) \quad (\text{Equation 5.2})$$

In the model, ε_w equals 80 under room temperature and ε_s usually equals 4 to 8. Consequently, the apparent dielectric constant Ka is mainly governed by the term $\varphi_w \varepsilon_w^\alpha$, which represents the impact of soil moisture, because ε_w is usually much higher than ε_s . Note that φ_w is the value of volumetric water content (θ), and φ_s can be calculated based on dry density (γ_d) and specific gravity of soil (G):

$$\varphi_s = V_s/V \quad (\text{Equation 5.3})$$

where V_s is the volume of soil particles, and V is the total volume of soil;

$$V_s = \frac{W_s}{G} = \frac{\gamma_d * V}{G} \quad (\text{Equation 5.4})$$

where W_s is the weight of soil particles, G is the specific gravity of soil particles, and γ_d is the dry density; so,

$$\varphi_s = \frac{\gamma_d}{G} \quad (\text{Equation 5.5})$$

The φ_s of three test sets and the differences of φ_s between groups shown are in Table 5.5.

Table 5.5: The volumetric portion of soil particles

Relative compaction	75%	80%	85%
---------------------	-----	-----	-----

φ_s	0.509	0.536	0.563
$\Delta\varphi_s$		0.027	0.027

The effects of φ_s and φ_w change on the reflecting period are summarized on Table 5.6. It was found that the sensitivity of reflecting period to the moisture portion is approximately one order of magnitude of that to the soil portion. This result validate the assumption of the three-phase model that the water content has a relative significant impact to dielectric properties of soil compared to soil particles.

Table 5.6: The effect of phase portion change on reflecting period

	φ_w from 0.27 to 0.37	φ_w from 0.17 to 0.27	φ_s increase 0.027
Change of phase portion $\Delta\varphi$	0.1	0.1	0.027
Change of reflecting period Δt (ms)	2	6	0.1
$\Delta t/\Delta\varphi$	20	60	3.7

Chapter 6: Effects of Temperatures on WCR Calibration Curves

6.1 OVERVIEW AND A TYPICAL RESULT

The specimens used in this series were prepared using only TYPE I method, which was presented in Chapter 4. This chapter presents the testing scope, results, and explanations of results, while the data interpretation will be presented in Chapter 7.

The specimens were tested in temperatures ranging from 40°C to -20°C, with a 5°C decrease between each two measurements, namely a total of 13 temperature points were acquired. The temperature control system constructed using a freezer and heating elements described in Chapter 4, permitted reaching the target temperatures. Table 6.1 shows the scope of the testing program.

Table 6.1: Scope of temperature correction testing program

Target temperature (°C)	Testing duration (hr)	Temperature error (°C)	Voltage of power supply (V)	Freezer (on/off)	Heating elements (on/off)
40	40	1	12.9	Off	On
35	>24	1	12.9	Off	On
30	>24	1	12.9	Off	On
25	>24	1	12.9	Off	On
20	>24	1	12.9	On	Off
15	>24	1	12.9	On	Off
10	>24	1	12.9	On	Off
5	>24	1	12.9	On	Off
1	>24	1	12.9	On	Off

-5	>24	1	12.9	On	Off
-10	>24	1	12.9	On	Off
-15	>24	1	12.9	On	Off
-20	>24	1	12.9	On	Off

Figure 6.1 shows a typical testing process. As can be seen, the process has 13 steps, each of which corresponds to a target temperature. The first step represents the temperature inside testing chamber rise from room temperature to 40 °C, where the reflecting period raised from 25 ms to 27.8 ms. Subsequently, after the WCR responses converging to a constant value, the setting temperature was lowered by 5°C, leading the specimen to reach a new equilibrium stage. At the end of each step, the reflecting period was record as the representative WCR responses of the specimen in that temperature. The illustration of equilibrium and selection of representative responses are summarized in Figure 6.2.

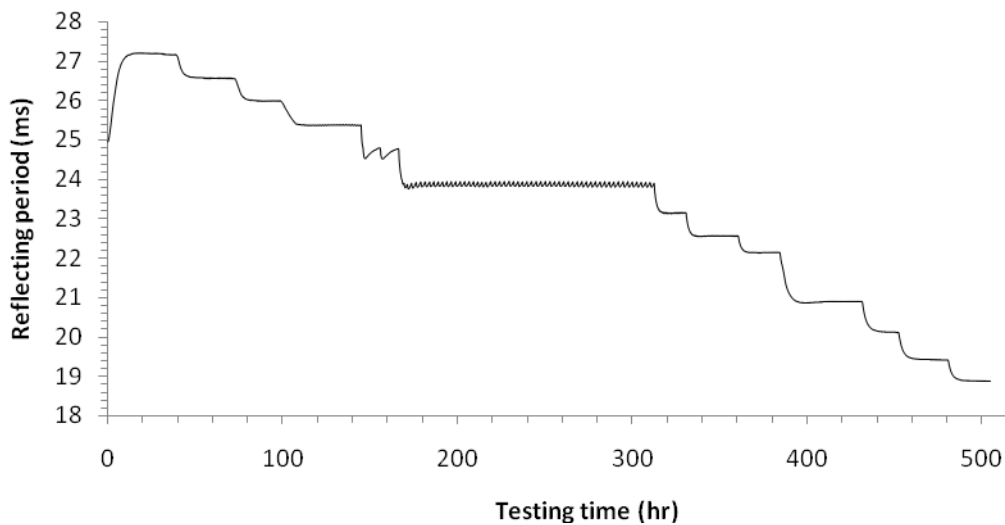


Figure 6.1: WCR responses in a graduate cooling test

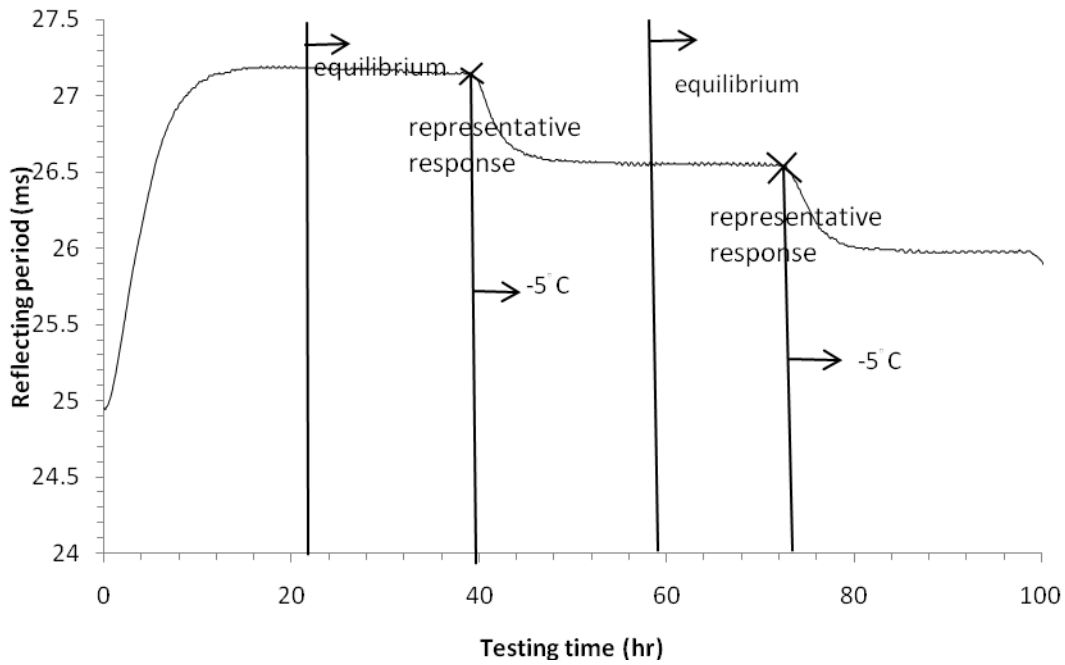


Figure 6.2: The equilibrium and representative response

6.2 SUMMARY OF WCR CALIBRATION RESULTS

The results from specimens of six different water contents in 13 different temperatures are presented in Table 6.2.

Table 6.2: Results of temperature correction tests

	Volumetric water content	Volumetric water content	Volumetric water content	Volumetric water content	Volumetric water content	Volumetric water content
	2.81%	10.89%	16.35%	21.61%	27.75%	33.62%
Temperature (°C)	Reflecting period (ms)	Reflecting period (ms)	Reflecting period (ms)	Reflecting period (ms)	Reflecting period (ms)	Reflecting period (ms)

40	17.41	27.17	33.95	38.4	40.34	42.4
35	17.34	26.55	33.2	37.68	39.77	42.05
30	17.28	25.98	32.43	36.88	39.06	41.59
25	17.2	25.36	31.59	36.02	38.23	41.03
20	17.09	24.655	30.42	34.78	37.045	40.28
15	16.98	23.87	29.12	33.42	35.52	39.05
10	16.88	23.14	27.9	32.04	33.99	37.72
5	16.78	22.56	26.93	30.82	32.72	36.11
1	16.7	22.14	26.2	29.91	31.7	34.99
0						
-5	16.59	20.9	23.01	24.24	23.38	24.23
-10	16.49	20.13	21.76	22.74	22.03	22.6
-15	16.38	19.44	20.82	21.69	21.02	21.5
-20	16.2	18.9	20.16	20.9	20.29	20.75

These data are summarized in Figure 6.3 in terms of reflecting period (t) and temperature (T). As can be seen, the reflecting period increases with increasing temperature, for each specimen of given volumetric water content. Additionally, an obvious decrease of reflecting periods can be observed when the temperature fell from 1 °C to -5 °C passing the freezing point of water (0 °C). The magnitude of the drop is a function of the volumetric water content. Specifically, the higher the volumetric water content of the specimen, the more significant is the decrease. For the specimen with volumetric water content of 2.8%, the drop is negligible and the WCR responses show an approximately continuous linear relation with the temperature. The phenomenon may be attributed to the drop of dielectric constant (ϵ_w) of water after freezing. Therefore, in the

driest specimen ($v_{mc}=2.8\%$), of which the portion of moisture is small, the impact of ϵ_w decrease on reflecting period is very small. The experimental results may validate the findings of Benson and Wang (2006), shown in Figure 2.12.

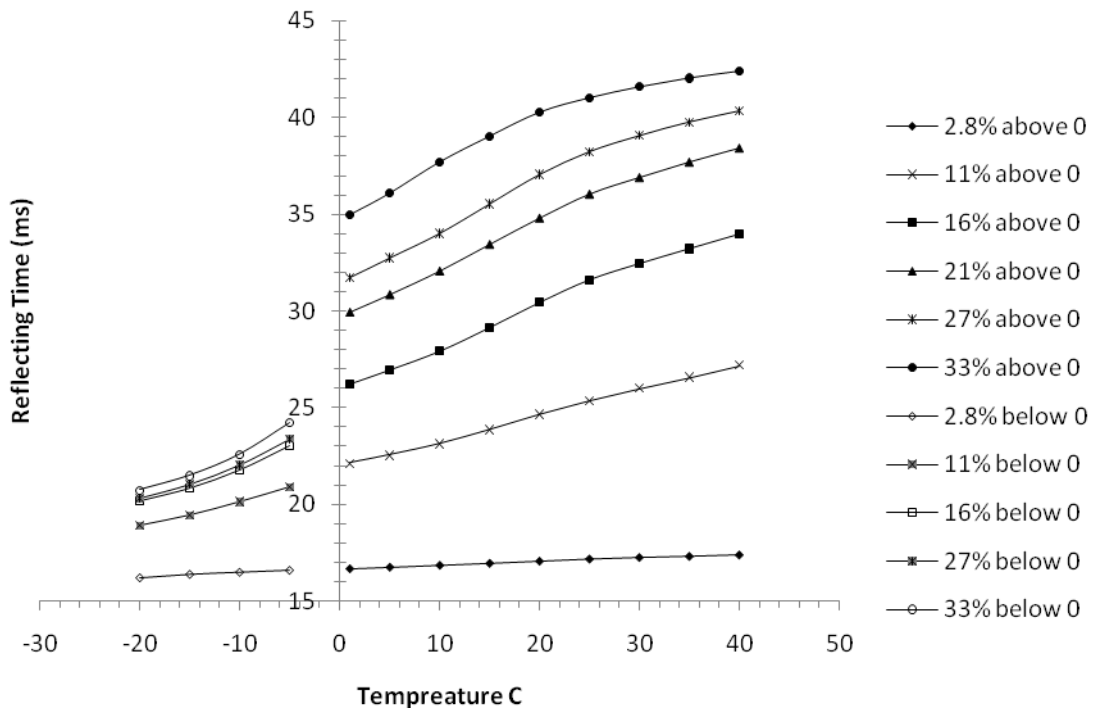


Figure 6.3: WCR responses for different temperatures and soil volumetric water content (2.8%, 11%, 16%, 21%, 27%, and 33%)

The temperature range goes across the water freezing point not only causing a drop of reflecting periods at the transition point, but also yielding a decrease of the effects of volumetric water content on reflecting period. That is, the difference of t between two different θ s in the range of positive temperatures is bigger than that in the range of negative temperatures. This phenomenon can be observed more clearly in Figure 6.4. The figure shows that the reflecting period (t) is a function of volumetric water content (θ) at

a given temperature. The reflecting period increases as the volumetric water content increases; this observation is consistent with the results presented in Chapter 5. Moreover, the changing rates of reflecting periods to volumetric water content are related to temperature; the $t-\theta$ curve of a high temperature is steeper than a curve of a low temperature. Nonetheless, the $t-\theta$ curves of temperatures that below 0°C are significantly shallower than the curves of temperatures that above 0°C . This relation also implies that the dielectric constant of water (ϵ_w) decrease significantly after freezing.

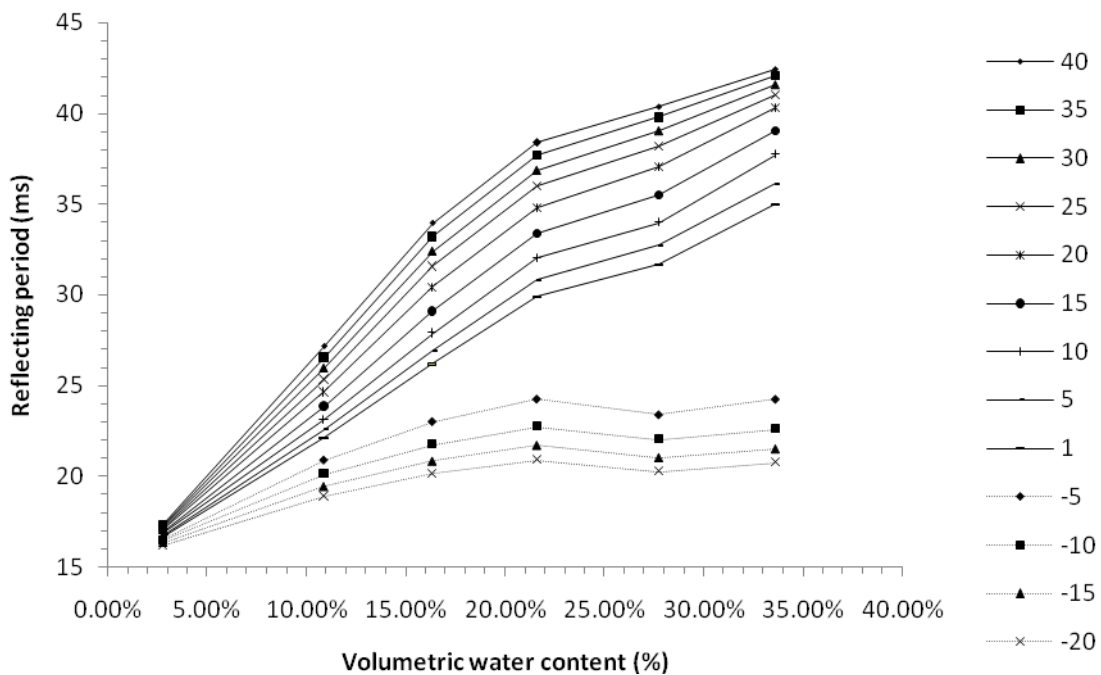


Figure 6.4: WCR responses for different volumetric water contents and temperature (40, 35, 30, 25, 20, 15, 10, 5, 1, -5, -10, -15, and -20 C)

Chapter 7: Interpretation of WCR Calibration Curves

7.1 OVERVIEW

This chapter interprets the results from the two series of tests stated above. Various curves and equations were used to fit the WCR responses with different relative compactions. Specifically, one set of equations was developed to fit the results from a given relative compaction with a single curve (Independent fit); another set of equations was developed to fit the results from all three sets of tests, and then variations were added on the equations to explain the density effect (Consolidated fit and shift). The approach and equations used to account for temperature effects on WCR calibrations are presented in section 7.3. An example of synthesizing both the response calibration and the temperature correction is presented in section 7.4.

7.2 INTERPRETATION OF WCR RESPONSE CURVES

7.2.1 Independent fit

Three sets of polynomial regressions (quadratic, cubic, and linear) were generated using data from each relative compaction group. The polynomial regressions were performed using the “Linest” function of Microsoft Excel. The R^2 values for each regression are also presented. R^2 is a statistical value for determining the effect of regression, which has a range from zero to one. A high R^2 value represents a good regression, while $R^2=1$ stands for a perfect regression.

Quadratic Regressions:

As recommended by the manufacturer, the volumetric water content (θ) and the reflecting period (t) was fitted to a quadratic polynomial:

$$\theta = C2 * t^2 + C1 * t + C0 \quad \text{(Equation 7.1)}$$

where t is the reflecting period (ms), θ is the volumetric water content, and Ci are regression coefficients.

The reflecting period obtained in dry air was used as a point where $\theta=0$ in quadratic regression. The regression coefficients and R^2 values are presented in Table 7.1. Curves based on the regression equations are presented in Figure 7.1. As shown in the figure, the three curves show relatively big errors at high θ compared to low θ . The porosities (n) of soil specimen are also shown in the figure, which represents the upper bound of volumetric water content.

Table 7.1: Quadratic polynomial coefficients and R^2 values

Relative compaction	75%	80%	85%
C0	-0.06479	0.047237	0.191317
C1	0.001334	-0.00898	-0.02255
C2	0.000224	0.000414	0.000653
R^2	0.984019	0.968725	0.999048

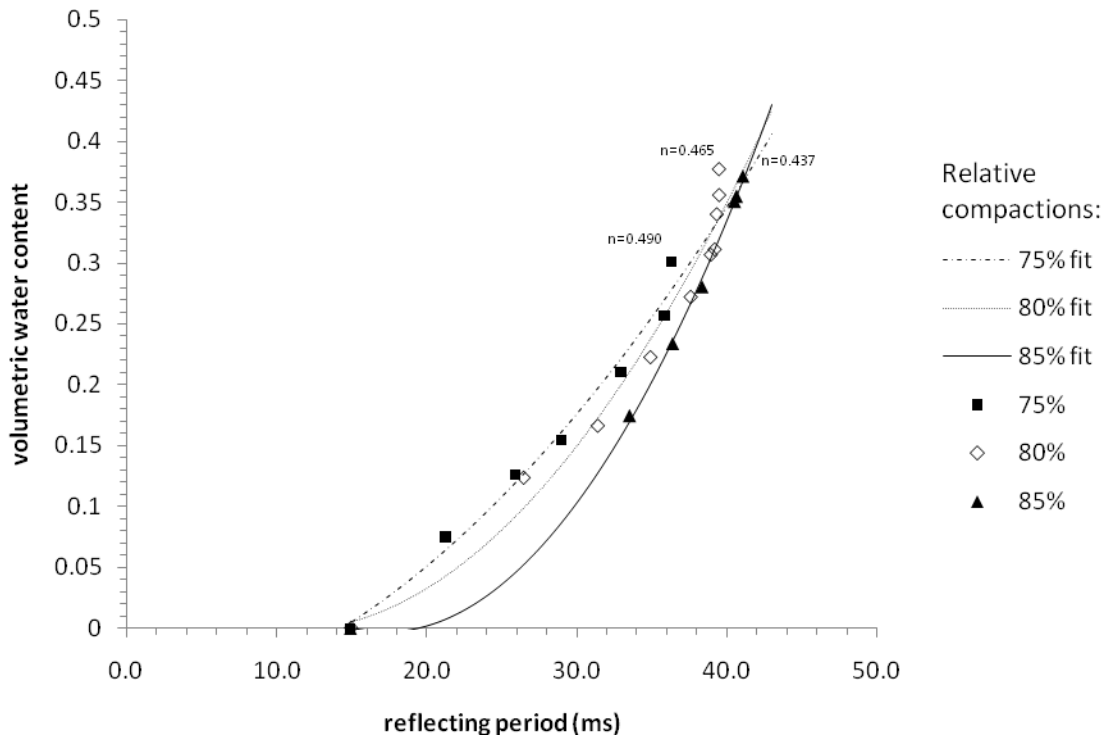


Figure 7.1: Quadratic fitting curves of different relative compactions

Cubic Regressions:

The volumetric water content and reflecting period were also fitted using a cubic polynomial:

$$\theta = C3 * t^3 + C2 * t^2 + C1 * t + C0 \quad \text{(Equation 7.2)}$$

where t is the reflecting period (ms), θ is the volumetric water content, and C_i are regression coefficients

The regression coefficients and R^2 values are summarized in Table 7.2. Curves based on the regression equations are illustrated in Figure 7.2. Compared to quadratic regression, the cubic curves generally fit the data better. The most striking aspect of cubic

curves is that they provide good prediction when θ is high compared to quadratic curves. Additionally, since the regression effect of cubic fit is good, it may provide a prediction of the corresponding reflecting periods in dry samples ($\theta = 0$).

Table 7.2: Cubic polynomial coefficients and R^2 values

Relative compaction	75%	80%	85%
C0	-1.65125	-5.38334	-7.24982
C1	0.183499	0.525953	0.606652
C2	-0.00655	-0.01683	-0.01699
C3	8.17E-05	0.000182	0.000164
R^2	0.986371	0.96839	0.999962

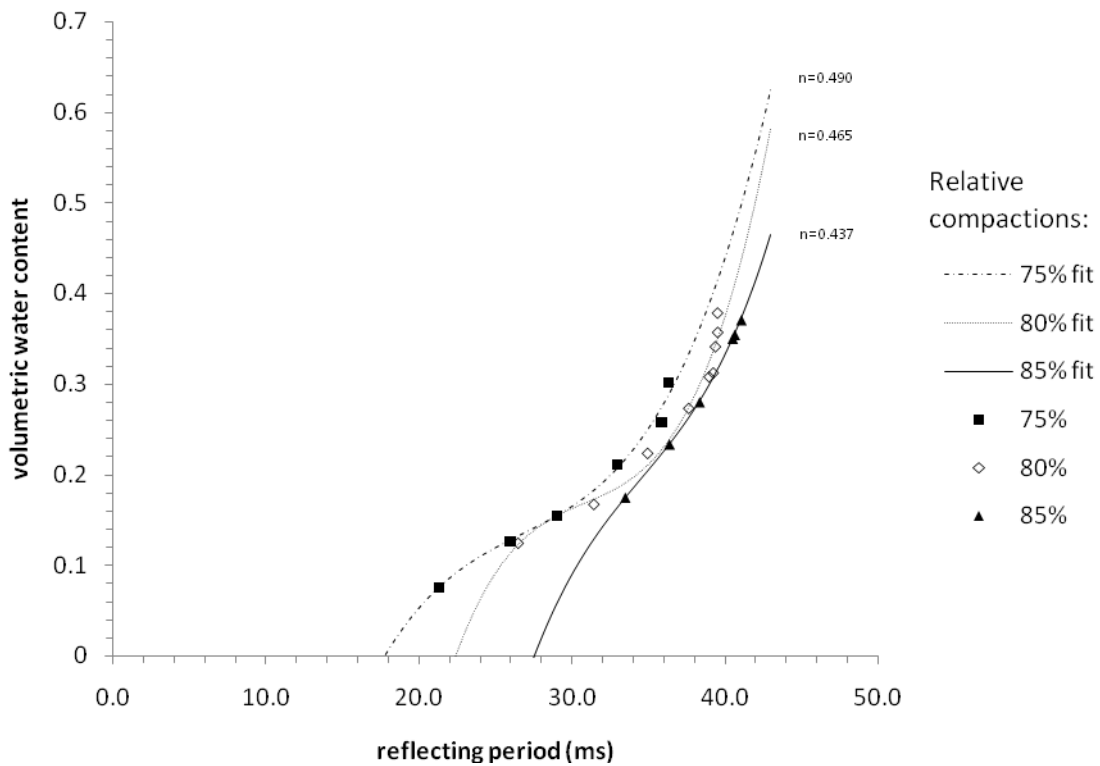


Figure 7.2: Cubic Fitting Curves of Different Relative Compactions

Linear Regressions:

Because the data points showed a linear trend where the relative compaction is 75%, the volumetric water content and reflecting period was fitted using a linear polynomial as well:

$$\theta = C1 * t + C0 \tag{Equation 7.3}$$

where t is the reflecting period (ms), θ is the volumetric water content, and Ci are regression coefficients.

The regression coefficients and R^2 values are presented in Table 7.3. Curves based on the regression equations are presented in Figure 7.3. The regression effects of linear polynomials are not as good as quadratic polynomials or cubic polynomials, but they provided acceptable predictions and easy calculations for dry density of 75% relative compaction.

Table 7.3: Linear Polynomial Coefficients and R^2 Values

Relative compaction	75%	80%	85%
C0	-0.20545	-0.24472	-0.22887
C1	0.013051	0.014402	0.013717
R^2	0.972566	0.930723	0.924351

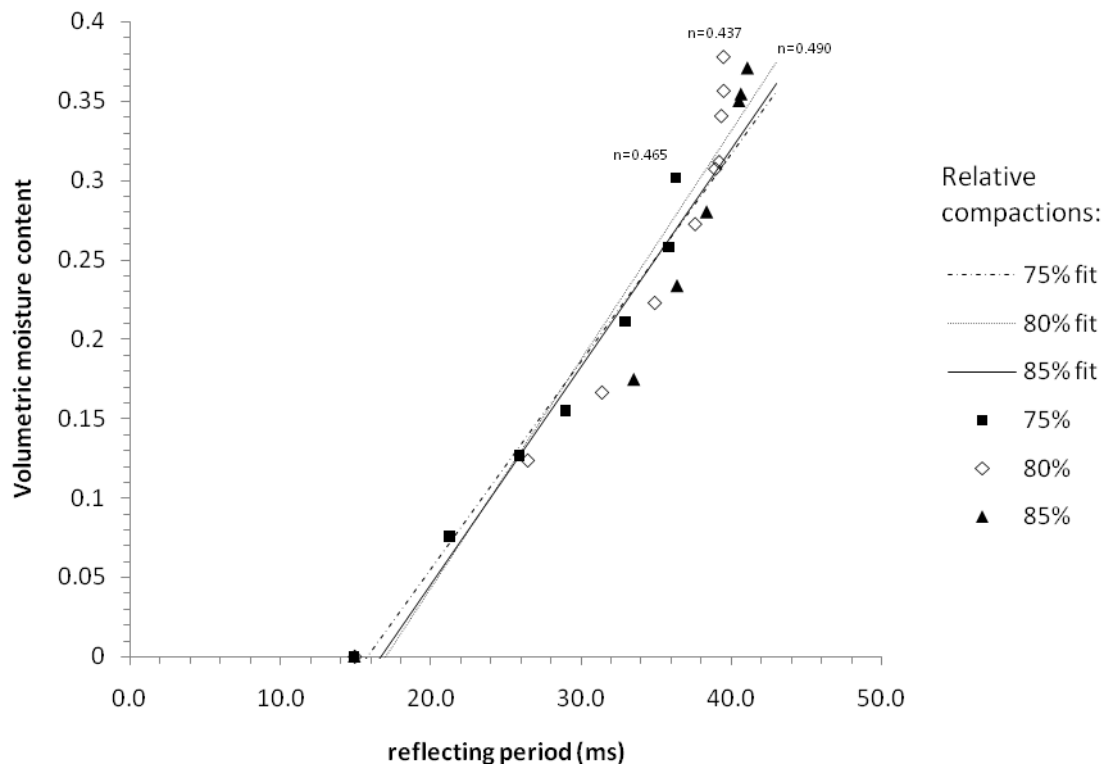


Figure 7.3: Linear fitting curves of different relative compactions

7.2.2 Consolidated fit and shift

A different method of regression called Consolidated Fit and Shift is presented in this section. Steps for performing Consolidated Fit and Shift are as follows:

- First, a polynomial regression is generated using data from all three data sets, which is called consolidated fit.
- Subsequently, a fit for 75% compaction group is looked for by only altering the constant coefficient in the consolidated fit equation, namely C_0 , which is called a shift from consolidated fit.
- Thirdly, the shifts for 80% and 85% compaction groups, which are the alteration of C_0 , are also looked for.

Totally, two sets of regression: quadratic and cubic, are conducted.

Quadratic regression:

The regression coefficients and R^2 values are summarized in Table 7.4. Curves based on the regression equations are presented in Figure 7.4. Note that the points where $\theta = 0$ was obtained in dry air. The relation of shifts and dry densities is presented in Figure 7.5.

Table 7.4: Coefficients of quadratic consolidated fit and shifts, and R^2 values

	Consolidated fit	shift 75%	shift 80%	shift 85%
C0	0.039109	0.054281	0.0416332	0.0231329
C1	-0.00678	-0.00678	-0.00678	-0.00678
C2	0.000358	0.000358	0.0003584	0.0003584
R^2	0.966895	0.975373	0.9284781	0.9763941

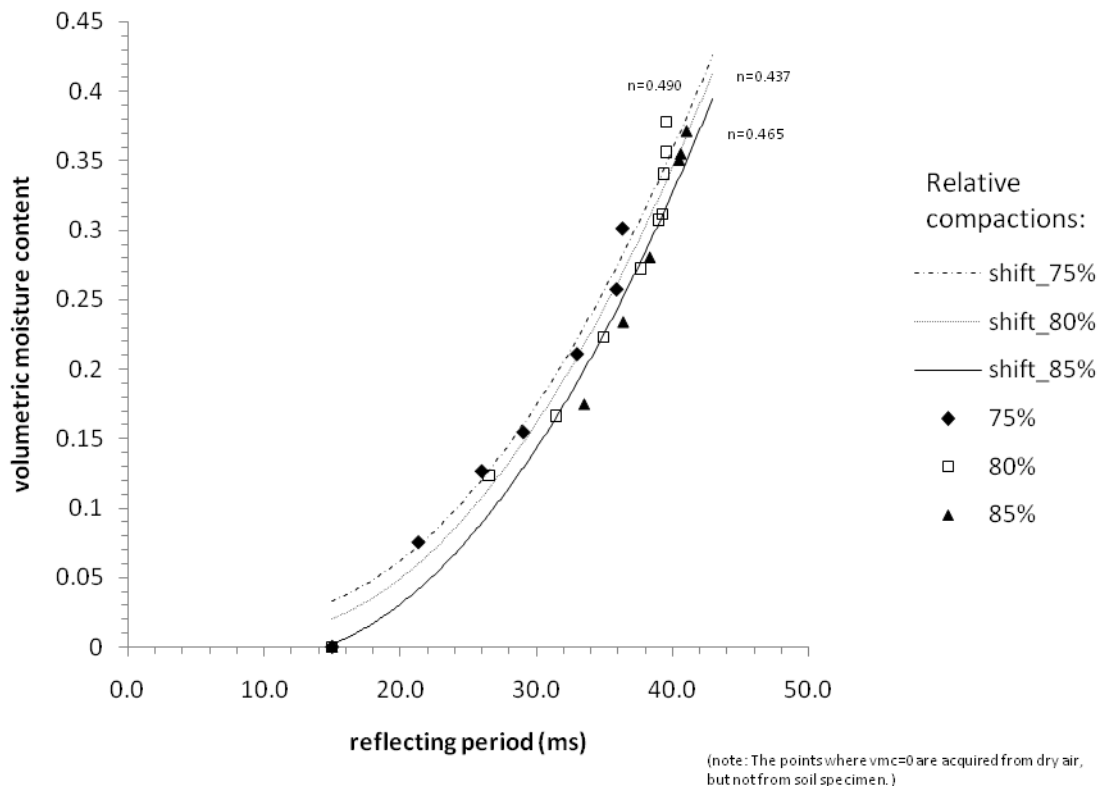


Figure 7.4: Curves of quadratic consolidated fit and shifts

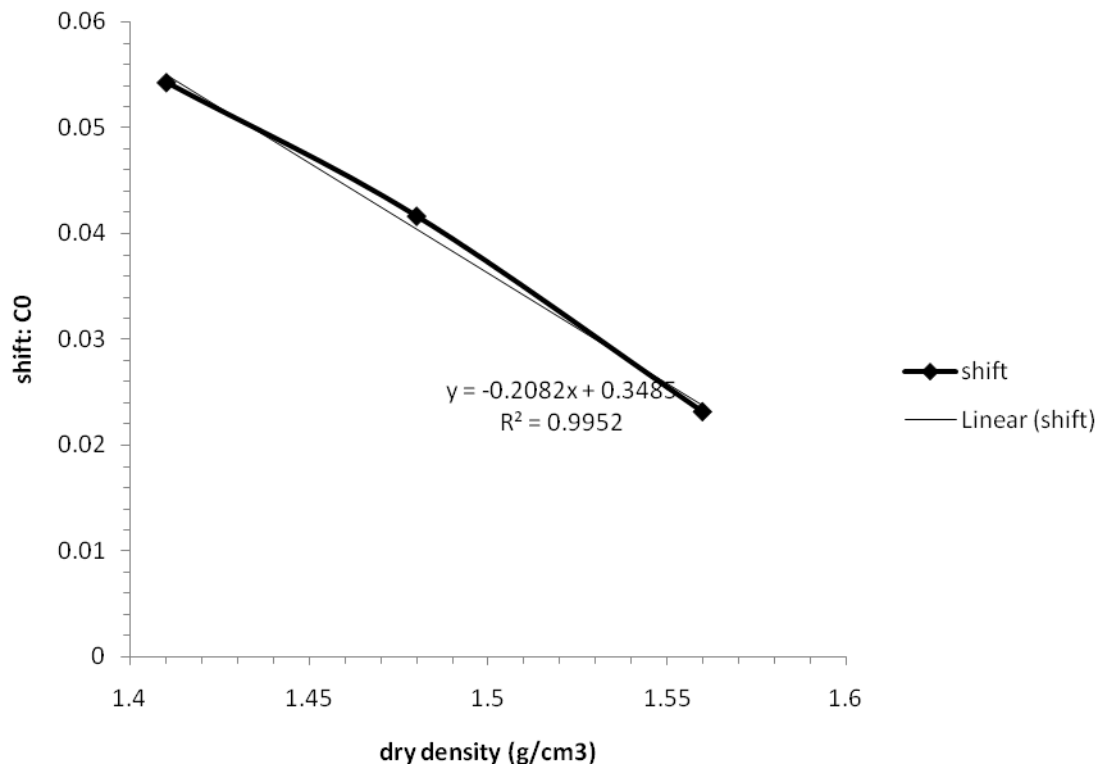


Figure 7.5: The relation of dry density and quadratic polynomial shift

Cubic regression:

The regression coefficients and R^2 values are presented in Table 7.5. Curves based on the regression equations are presented in Figure 7.6. Note that the points where $\theta = 0$ are acquired in dry air. The relation of shifts and dry densities is presented in Figure 7.7.

Table 7.5: Coefficients of cubic consolidated fit and shifts, and R^2 values

	Consolidated fit	shift 75%	shift 80%	shift 85%
C0	-0.52137	-0.50804	-0.51846	-0.53907
C1	0.059741	0.059741	0.059741	0.0597

C2	-0.00209	-0.00209	-0.00209	-0.00209
C3	2.85E-05	2.85E-05	2.85E-05	2.85E-05
R ²	0.975275	0.960173	0.951248	0.992747

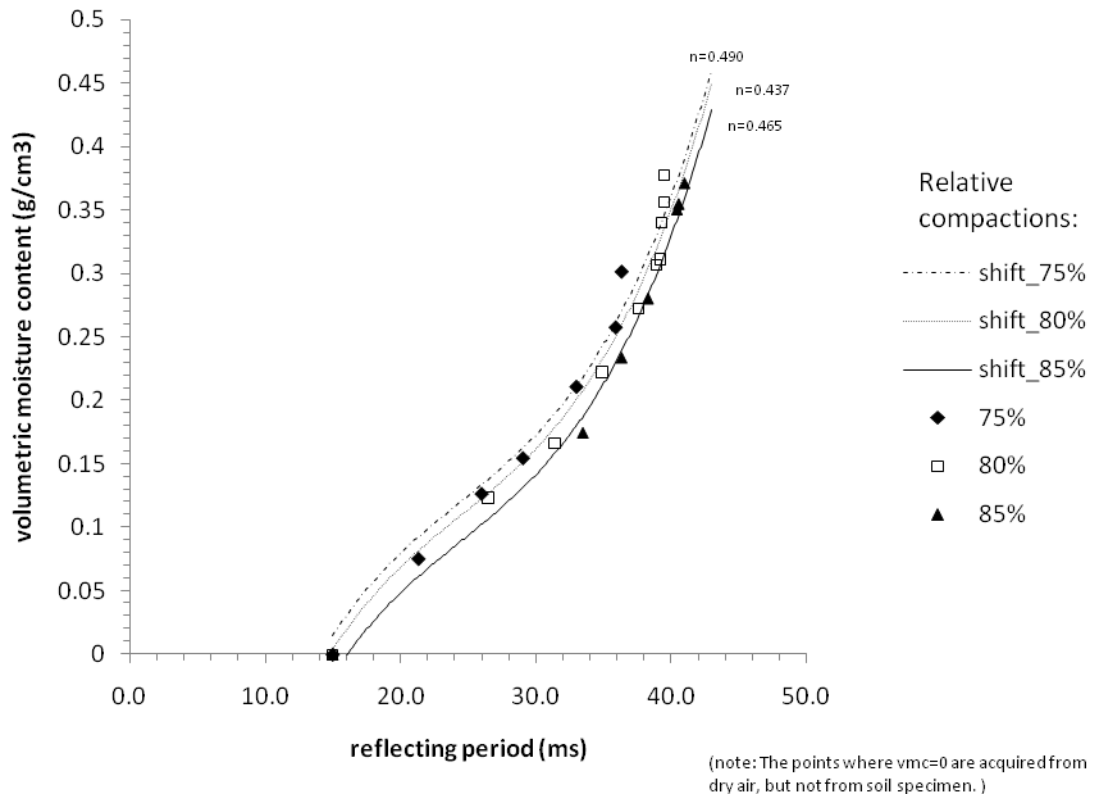


Figure 7.5: Cubic consolidated fit and shifts

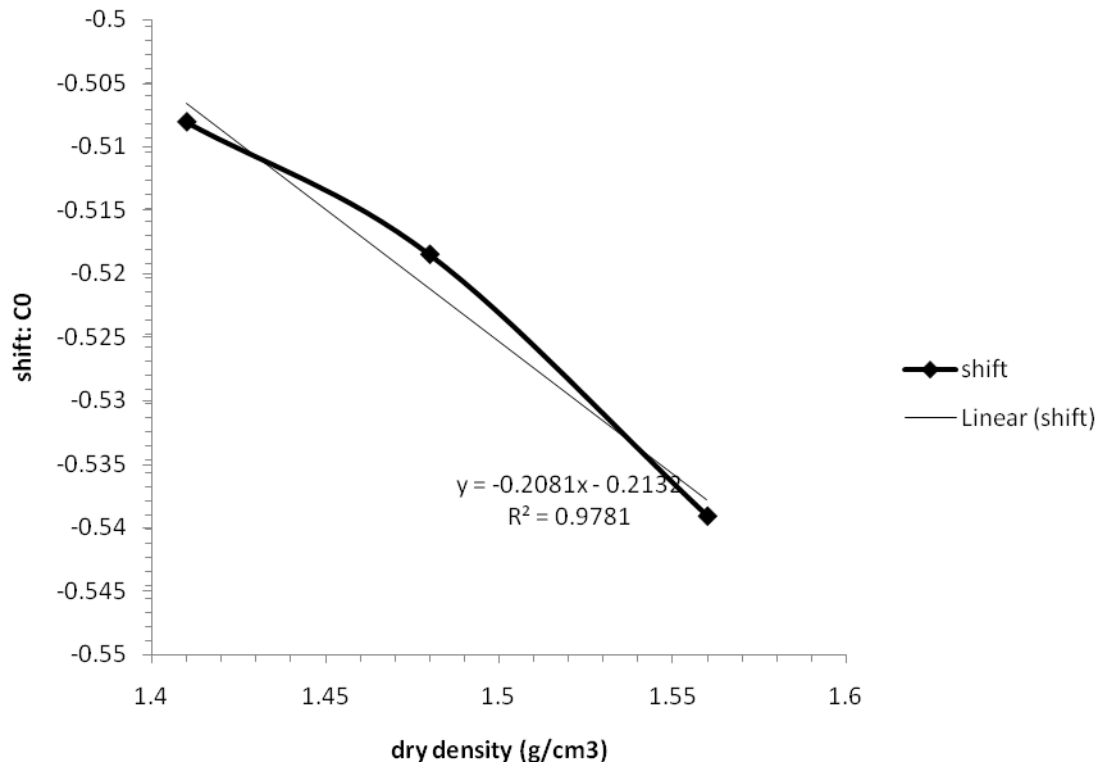


Figure 7.7: The relation of dry density and cubic polynomial shifts

Prediction of shift value for other densities:

Because the relations of shifts and dry densities showed linear trends, as shown in Figure 7.5 and Figure 7.7, a shift could be predicted, and keep the other coefficients unchanged, to generate a new equation for a dry density value that was beyond the testing scope in this study.

For example, the soil at one site has a dry density of 1.60g/ cm³; field engineers insert a WCR into the soil, the reading is 29.05ms.If we decide to use a cubic consolidated and shift equation to predict the volumetric water content, the steps are listed:

1. Density (g/cm³): x=1.6
2. Shift: y=-0.2081x-0.2132=-0.54616
3. C0=y=-0.54616; C1=0.069741; C2=-0.00209; C3=2.85×10⁻⁵
4. $\theta = C3 \cdot t^3 + C2 \cdot t^2 + C1 \cdot t + C0 = 0.1242$

7.3 INTERPRETATION OF TEMPERATURE CORRECTION EQUATIONS

The aim of temperature correction is correcting a reflecting period measured under a random temperature that is different from the standard temperature used to define the calibration curve (section 7.2). As stated in Chapter 6, the WCR response (reflecting period) increases as the soil temperature increases. However, the WCR responding calibration equation, through which the volumetric water content (θ) is derived from reflecting period (t), is generated under standard temperature. To apply any calibration equation, the reflecting period (t) in field temperature needs to be converted to a corresponding value in a standard temperature, in which the calibration equation is generated. For this purpose, Campbell Sci. presented a temperature correction equation (Campbell Sci., 2002):

$$t_{corrected} = t_{uncorrected} + (20 - T)(0.526 - 0.052 * t_{uncorrected} + 0.00136 * t_{uncorrected}^2)$$

(Equation 7.4)

where, $t_{corrected}$ is the corrected reflecting period at 20°C (ms), T is the soil temperature (°C), and $t_{uncorrected}$ is the original reflecting period (ms). This equation was obtained from

experiments performed at various water contents and over temperatures ranging from 10°C to 40°C (Campbell Sci., 2002).

In this study, the standard temperature for correction is also selected to be 20°C. The approach of correction is illustrated in Figure 7.8. In this figure, a three dimensional space, which has the axes of temperature (T), reflecting period (t), and volumetric water content (θ), is constructed. The shaded meshes represent the database from the experimental results in this study, as presented in Chapter 6; the white meshes represent the temperature correction of Campbell Sci., of which the temperature range has been extended to -20°C~40°C. The square markers stand for measurements taken in various temperatures. Assuming that a perfect temperature correction is performed, the round markers stand for corrected measurements in 20°C. As can be seen, each corrected measurement has the same value of volumetric water content with its original uncorrected one.

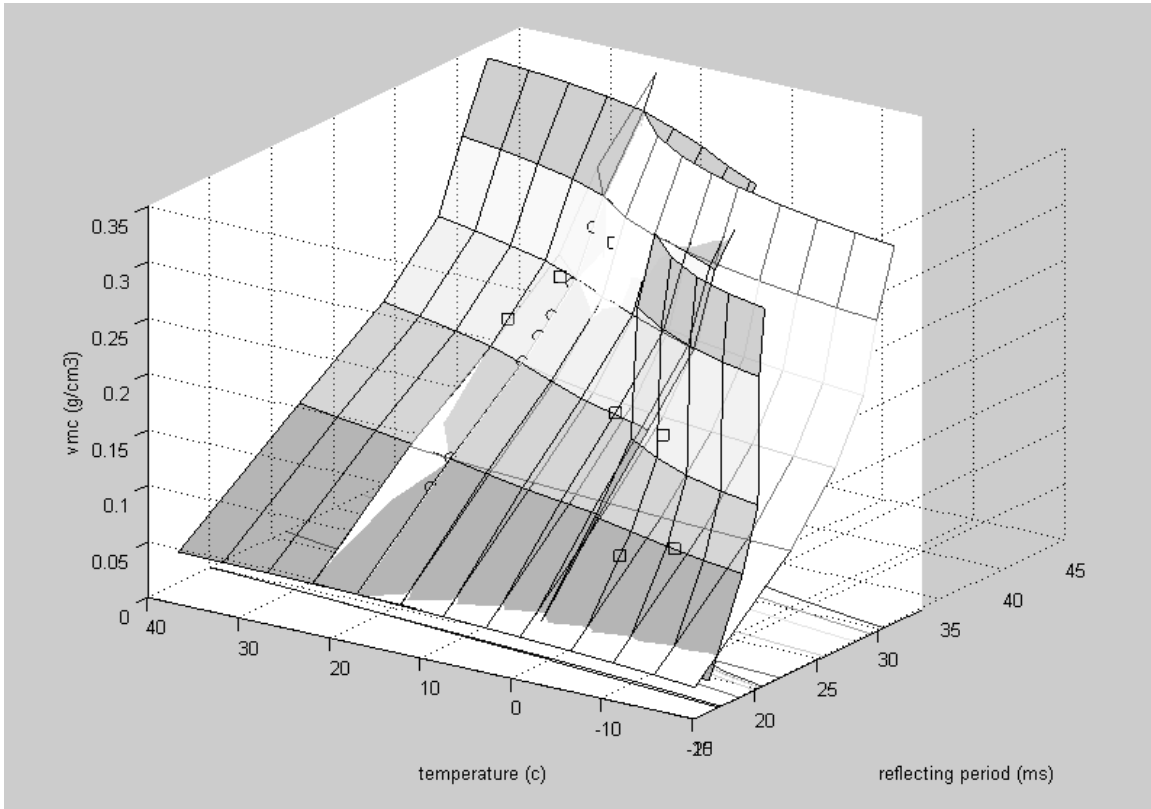


Figure 7.8: Temperature correction database: A 3-D view

In this study, temperature correction is performed respectively in three regions: -20~0°C, 0~ 20°C and 20~40°C. Examining the shape of curves that illustrated WCR responses in different temperatures, presented in Figure 6.3, one can notice that there is a significant difference between the measurements below and above 0°C. Moreover, the slopes of curves are likely shallower above 20°C than those ranging from 0 to 20°C. Consequently, the temperature range was separated into three regions: -20~0°C, 0~ 20°C and 20~40°C; and temperature correction was generated in each region individually.

In each region, the form of the correction equation is:

$$t_{corrected} = t_{uncorrected} + (T_{std} - T)(a_0 - a_1 * t_{uncorrected} + a_2 * t_{uncorrected}^2)$$

(Equation 7.5)

where $t_{corrected}$ is the corrected reflecting period at T_{std} (ms), T is the soil temperature ($^{\circ}\text{C}$), T_{std} is the standard temperature ($^{\circ}\text{C}$), $t_{uncorrected}$ is the original reflecting period (ms), and a_0 , a_1 , and a_2 are correction parameters.

For the 20~40 $^{\circ}\text{C}$ region, parameters are summarized in Table 7.6. The correction effects are illustrated in Figure 7.9. In the figure, each curve represents a specimen at given water content. Curves with names as “*%” represent the original experimental results; curves with names as “*%crt” represent the corrected reflecting periods. Because the standard temperature is 20 $^{\circ}\text{C}$, the corrected value in 20 $^{\circ}\text{C}$ should be the same as the original value. Moreover, the corrected values in other temperatures should be the same as that in 20 $^{\circ}\text{C}$ if the correction is perfect, because they are at the same water contents. As a result, the corrected curves should be horizontal lines. As shown in Figure 7.9, the corrected curves are likely adequate level, indicating the correction effect could be considered acceptable.

Table 7.6: Correction parameters (20-40 $^{\circ}\text{C}$)

T_{std} ($^{\circ}\text{C}$)	a_0	a_1	a_2
20	-0.54335	0.042827	-0.00063

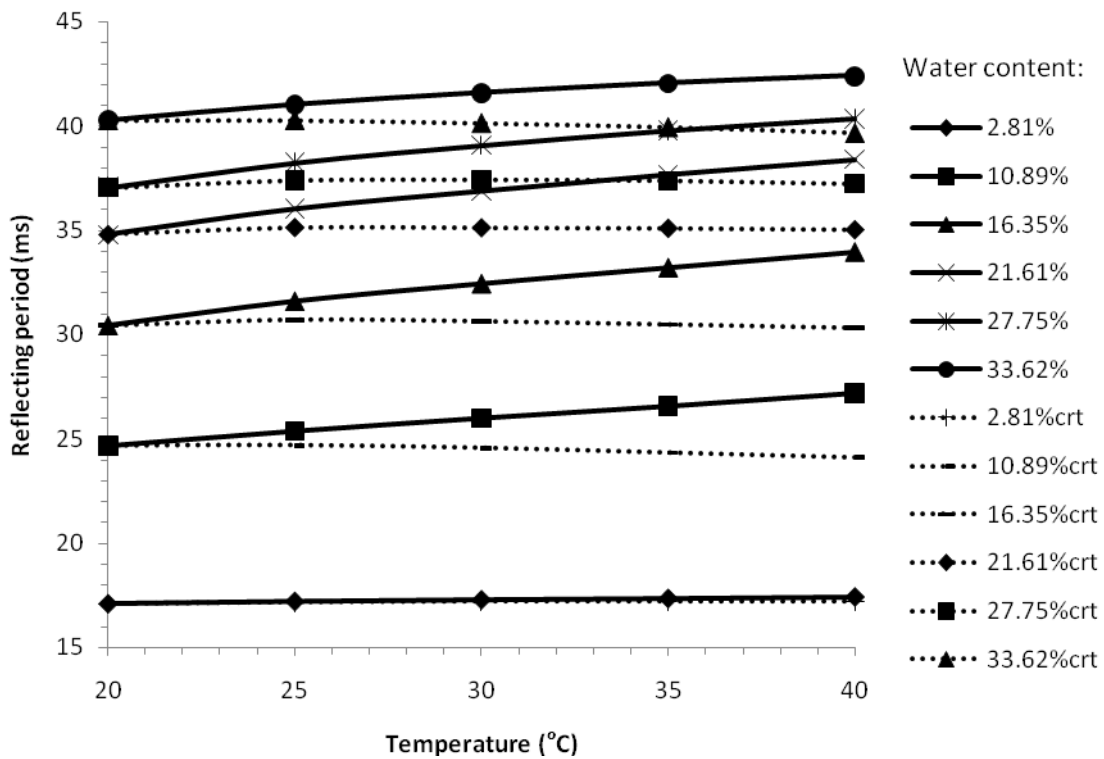


Figure 7.9: Temperature correction effect in temperature of 20-40°C

For the 0~20°C region, correction parameters are summarized in Table 7.7. Figure 7.10 shows the correction effect of temperature correction. In the figure, corrected curves are likely level and share the same value as those at 20°C, implying that the correction effect is satisfactory.

Table 7.7: Correction parameters (0-20°C)

T_{std} (°C)	a0	a1	a2
20	-0.682	0.054453	-0.00077

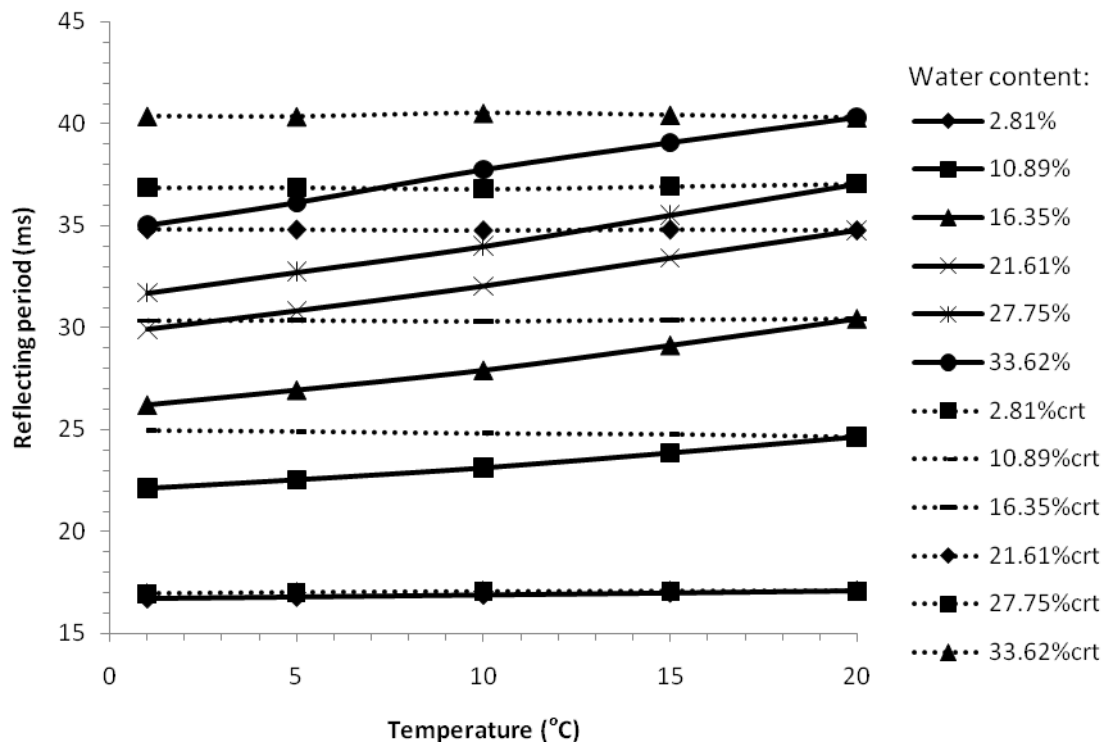


Figure 7.10: Temperature correction effect in temperature of 0-20°C

For the -20~0°C region, the correction steps were modified in order to make the results compatible with those in regions 0~20°C and 20~40°C.

First, the reflecting periods were corrected to corresponding values at -5°C using the form as manufacturer's equation. The correction parameters are summarized in Table 7.8.

Table 7.8: Correction parameters (-20-0°C)

T_{std} (°C)	a0	a1	a2
-5	-0.18818	-0.01101	0.001484

Subsequently, the corrected periods at -5°C (t_{-5}) are converted to a corresponding value (t_{20}) at 20°C , using a converting equation as:

$$t_{20} = -497.68 + 80.314 \cdot t_{-5} - 4.2154 \cdot t_{-5}^2 + 0.075 \cdot t_{-5}^3 \text{ (Equation 7.6)}$$

The correction effect is shown in Figure 7.11. As can be seen, the corrected curves show horizontal trends though they are not as level as those shown in Figure 7.9 and Figure 7.10.

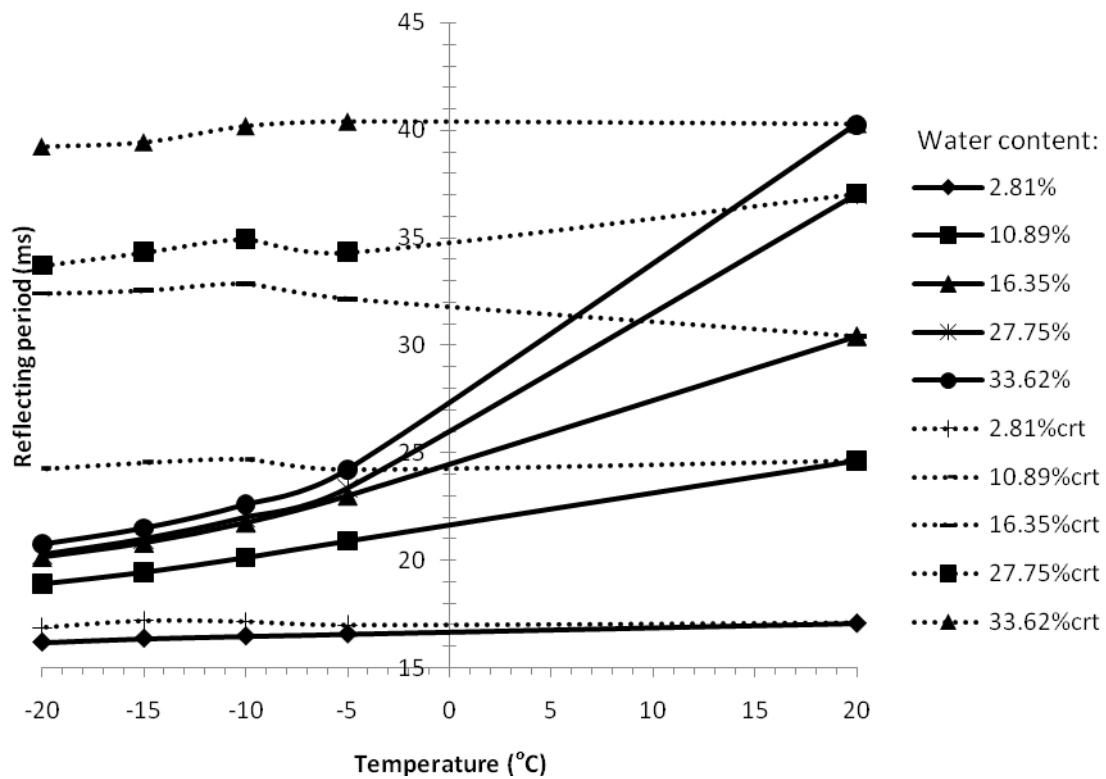


Figure 7.11: Temperature correction effect in temperature of -20 - 0°C

7.4 SYNTHESIZED APPLICATION OF RESPONSE CALIBRATION AND TEMPERATURE

CORRECTION

Assuming a set of measurements was taken under nine temperatures (1, 5, 10, 15, 20, 25, 30, 35, and 40°C) in RMA with relative compaction of 80%, the reflecting periods were found to be 20ms, 25ms, 30ms, 35ms, and 40ms at each temperature. Namely, a total of 45 measurements were recorded.

The prediction of volumetric water contents using the Quadratic Consolidated Fit and Shift method and temperature correction is summarized in Figure 7.12 and Figure 7.13. The two figures show volumetric water content as a function of temperature and as a function of reflecting period respectively. As shown in the figures, for a given temperature, the prediction of θ increases as the reflecting period increases (t); the increasing rate of θ with t decreases with increasing temperature (T). Additionally, for a given reflecting period, the prediction of θ decreases as the temperature increases; the decreasing rate of θ with T increases with increasing reflecting period (t).

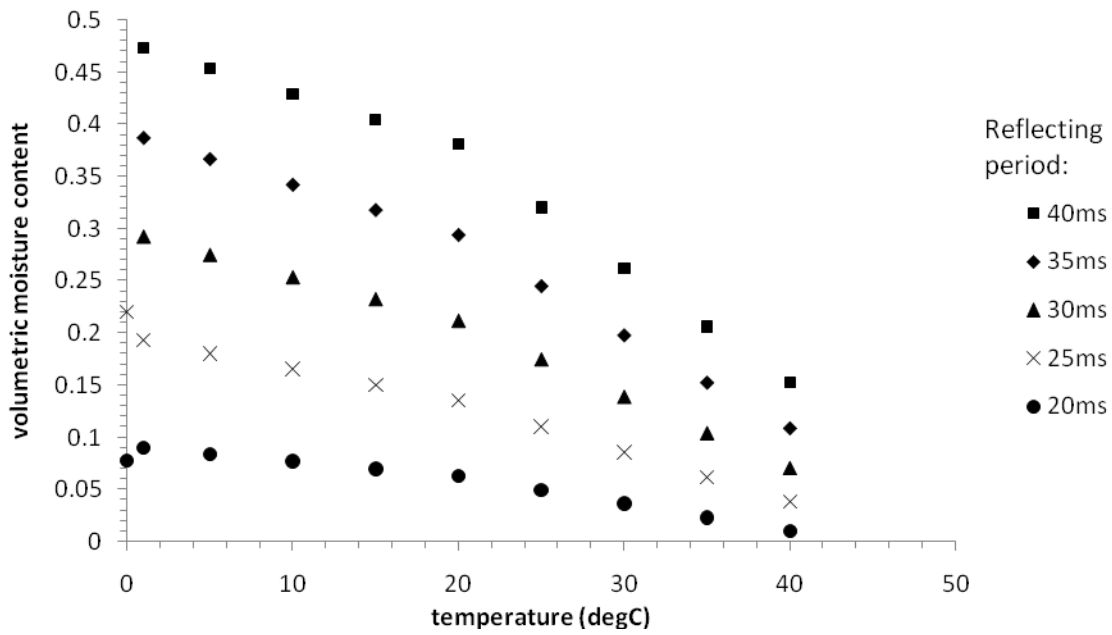


Figure 7.12: volumetric moisture content as a function of temperature with the corresponding reflecting period of 40, 35, 30, 25, 20, and 15ms

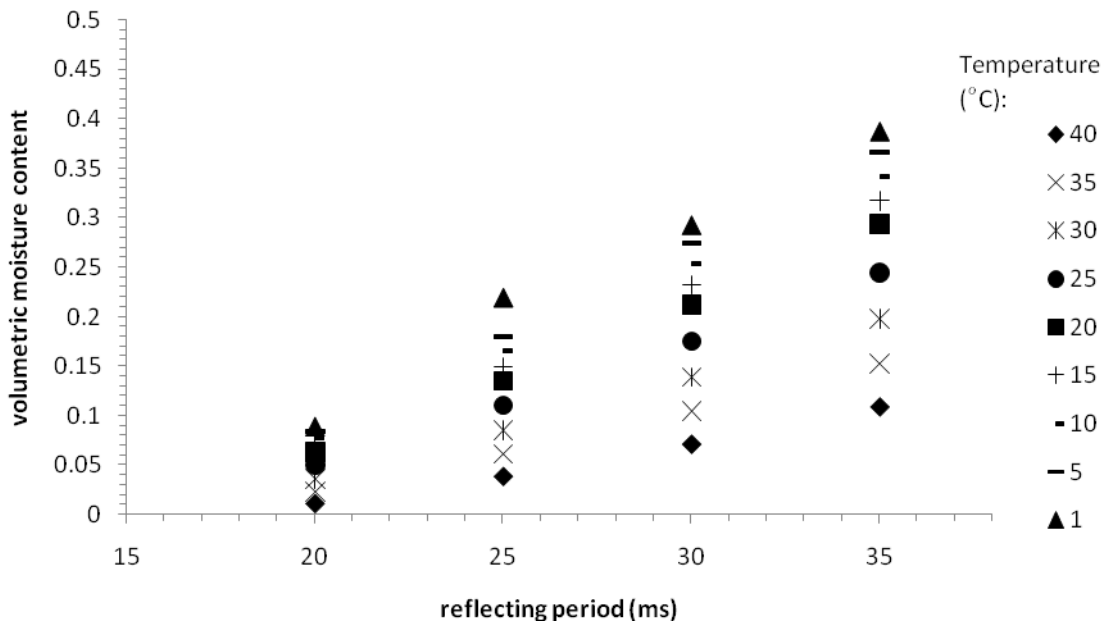


Figure 7.13: volumetric moisture content as a function of reflecting period in the temperature of 40, 35, 30, 25, 20, 15, 10, 5 and 1°C

Chapter 8: Applications of Calibration Results

8.1 OVERVIEW

This chapter presents a comparison between the WCR calibration in this study and the manufacturer's calibration equation. A comparison in temperature correction is also presented. A field problem, which is of the same soil type, is described; a comparison in predicting in-situ water content between using the temperature correction in this study and using the correction recommended by manufacturer is also shown.

8.2 COMPARISON BETWEEN THE RESPONSE CURVE IN THE STUDY AND MANUFACTURER'S RESPONSE CURVE

Campbell Sci. (2002) derived a WCR calibration, based on measurements in a loam soil with bulk density 1.4g/cm^3 :

$$\theta = -0.0663 - 0.0063 * t + 0.0007 * t^2 \quad (\text{Equation 8.1})$$

A comparison between the experimental results in the study and Campbell Sci. equation is shown in Figure 8.1. As can be seen, the predicting volumetric water content for a given reflecting period from manufacturer's equation is generally higher than the experimental results in the study. This discrepancy may be mainly attributed to the difference of bulk density. In this study, the dry densities of specimen are 1.41, 1.485, and 1.56 g/cm^3 ; the corresponding bulk densities at various θ are summarized in Table 8.1.

Table 8.1: bulk densities and volumetric water contents

	$\rho_d = 1.41 \text{ g/cm}^3$	$\rho_d = 1.485 \text{ g/cm}^3$	$\rho_d = 1.56 \text{ g/cm}^3$
	$\rho \text{ (g/cm}^3\text{)}$	$\rho \text{ (g/cm}^3\text{)}$	$\rho \text{ (g/cm}^3\text{)}$
$\theta = 0.1$	1.51	1.585	1.66
$\theta = 0.2$	1.61	1.685	1.76
$\theta = 0.4$	1.81	1.885	1.96

As shown in the table, the bulk densities of soil specimens are generally higher than that of manufacturer's data base (1.40). As a result, manufacturer's equation might overestimate the volumetric waters for denser soils. This finding is compatible with the literature review stated in section 2.3.5.

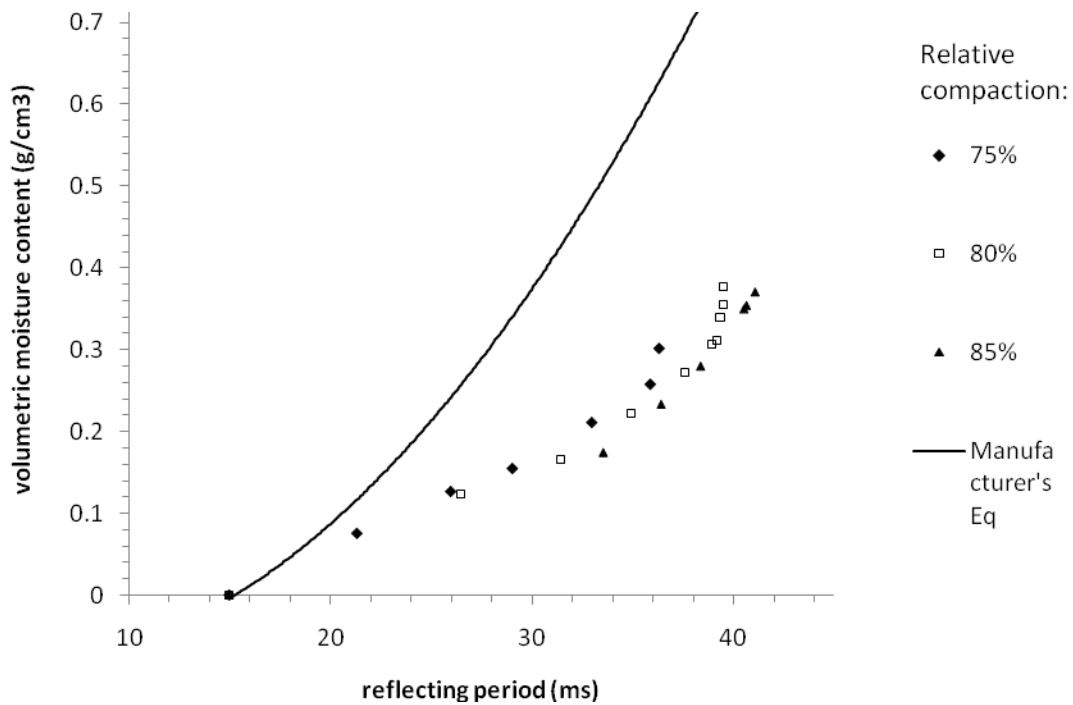


Figure 8.1: Comparison of the WCR responses results in this study and the manufacturer's equation

8.3 COMPARISON BETWEEN THE TEMPERATURE CORRECTION CURVES IN THE STUDY AND MANUFACTURER'S TEMPERATURE CORRECTION

Comparisons of the temperature correction in the study and the temperature correction provided by manufacturer under different temperatures (30°C, 15°C, and 1°C) are presented in Figure 8.2, Figure 8.3 and Figure 8.4. The figures illustrated the relations of uncorrected reflecting time and corrected reflecting for both two temperature correction equations. Discrepancies are observed at high uncorrected reflecting time portion (also known as high volumetric water content portion) in all three figures. Additionally, a discrepancy along the total range of reflecting time is observed between the curves of 1°C. The finding may be attributed to the limited temperature range (10°C-40°C) of manufacturer's testing program.

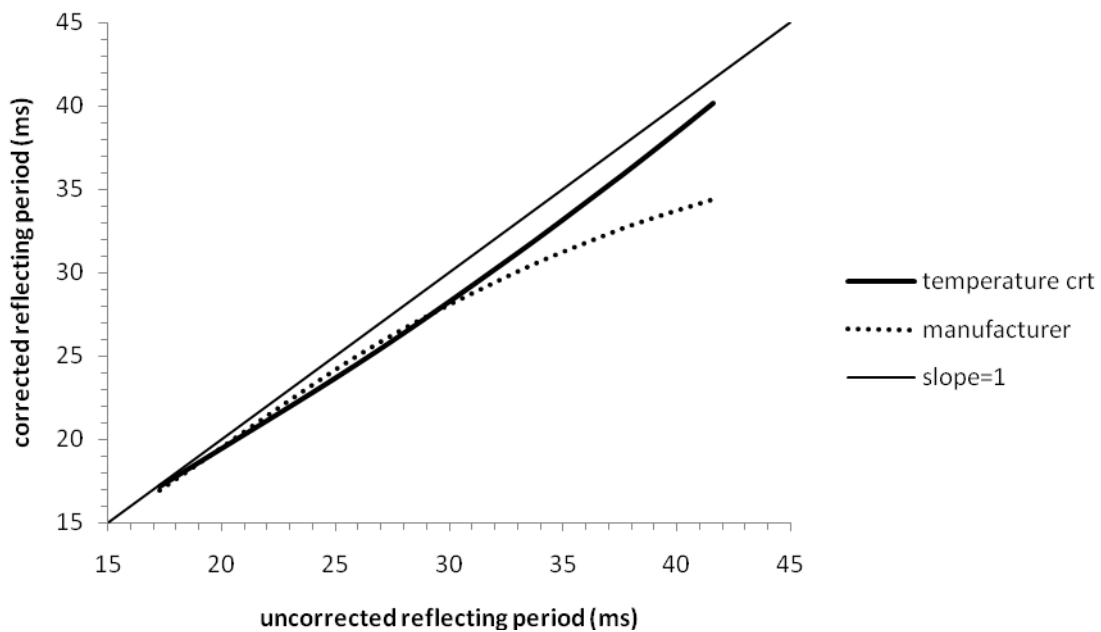


Figure 8.2 Temperature correction comparison (30°C)

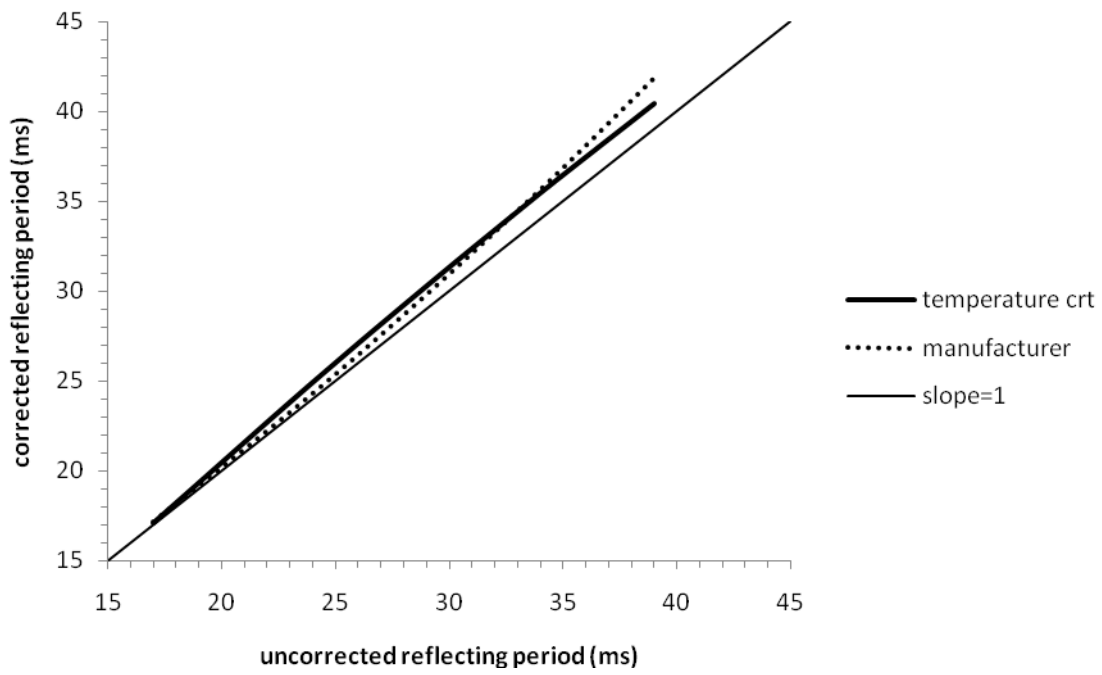


Figure 8.3 Temperature correction comparison (15°C)

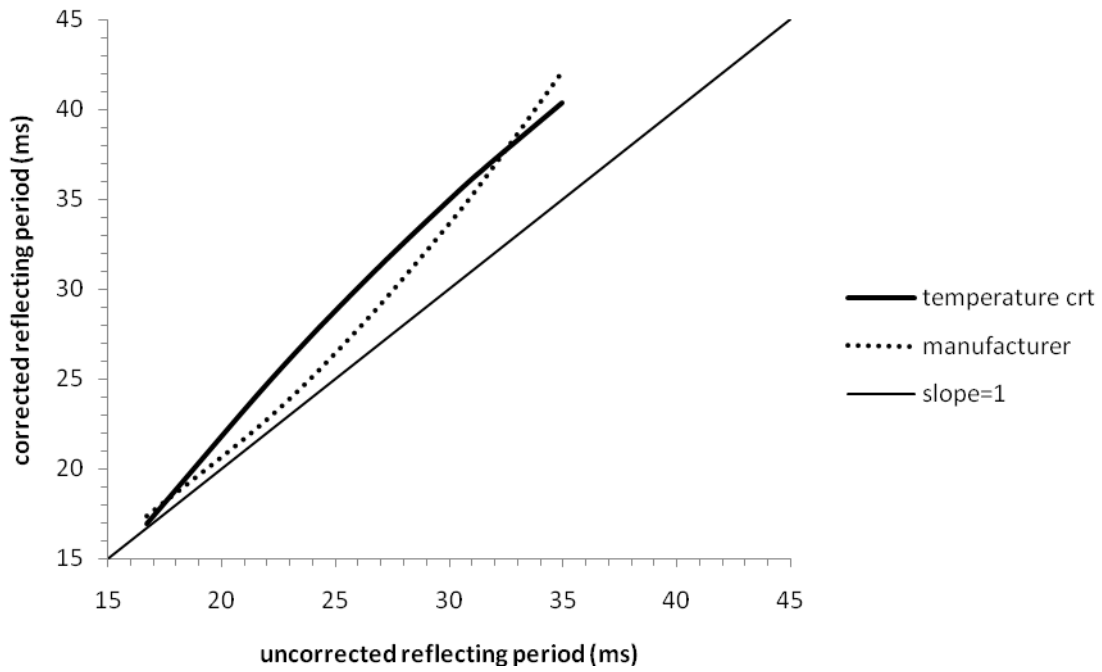


Figure 8.4 Temperature correction comparison (1°C)

8.4 APPLICATIONS OF THE TEMPERATURE CORRECTION

Results from an in-situ monitoring study involving soil moisture was used show the use of the temperature correction defined in this study. In the field, WCRs were installed in different depths in a landfill cover system, which was made of similar compacted RMA soil.

A moisture monitoring record is presented in Figure 8.5. This is a record of from probes located at the lowest elevation in the site, where the soil was wetted from September 2007 to July 2008, and naturally dried out from then on. In this figure, moisture contents were calculated using manufacturer's temperature correction. Because the probes are installed at the base of the cover, by investigating the precipitation records and the reflecting periods taken from WCRs at upper depths, it is deducted that the soil at this layer has reached saturation from October 2007, and maintained this condition till the dry out started. For this reason, the curves should stay at a constant value, which should equal to the porosity (n) of the soil, from during October 2007 to July 2008. However, the curves showed fluctuations or concaves during this period in Figure 8.6.

Figure 8.6 is reconstructed from Figure 8.5 using the temperature correction in this study from the same record. As can be seen, the moisture content records maintain a likely level trend during Oct 2007- Jul 2008. This trend is consistent with the deduction above. Thus the temperature correction may be more suitable for predicting moisture in RMA soil than the manufacturer's equation. Figure 8.7 shows a comparison of the data corrected using both two methods. The figure shows that the temperature correction defined in this study generates a prediction that fits better the deduction stated above.

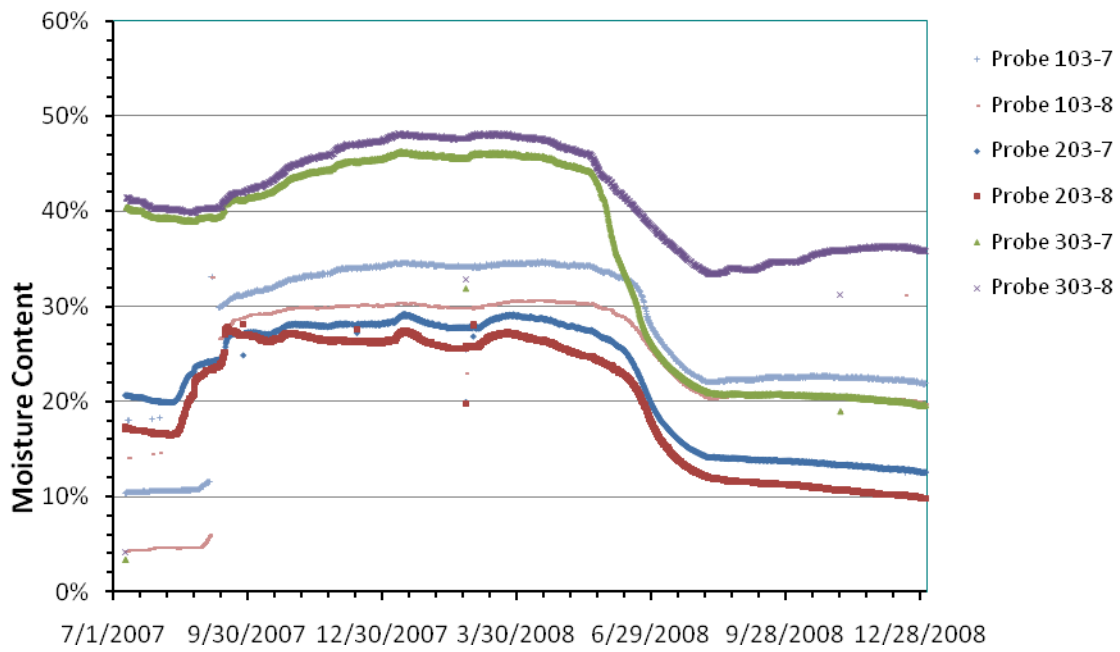


Figure 8.5: An application using manufacturer's temperature correction equation to a field

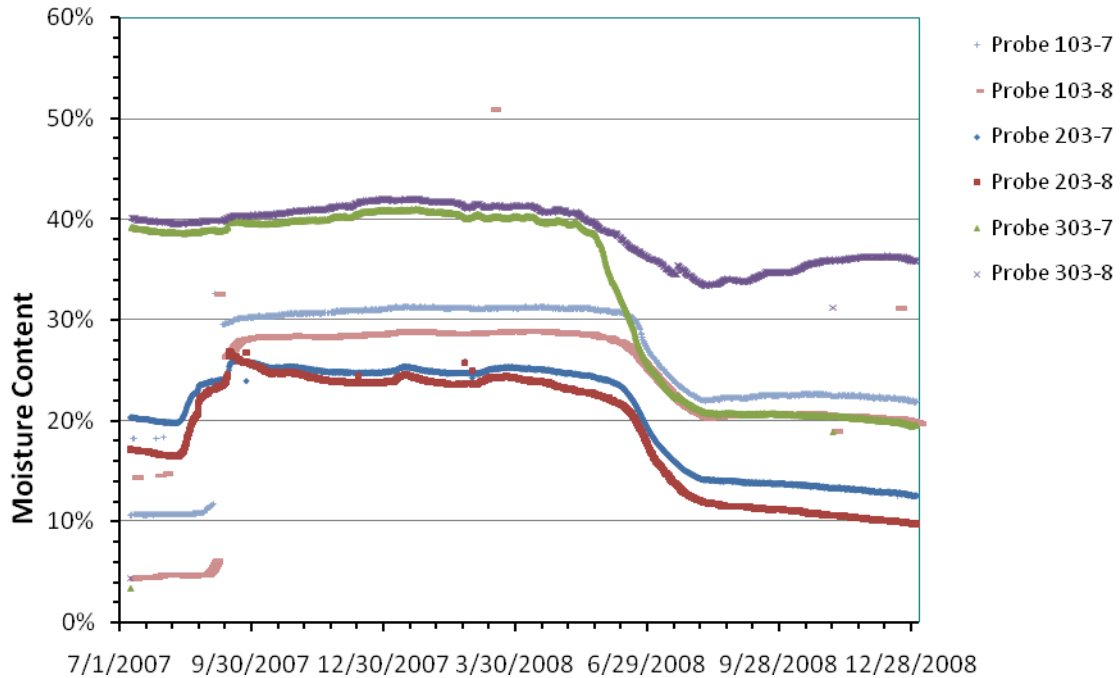


Figure 8.6: An application using the temperature correction in this study to a field

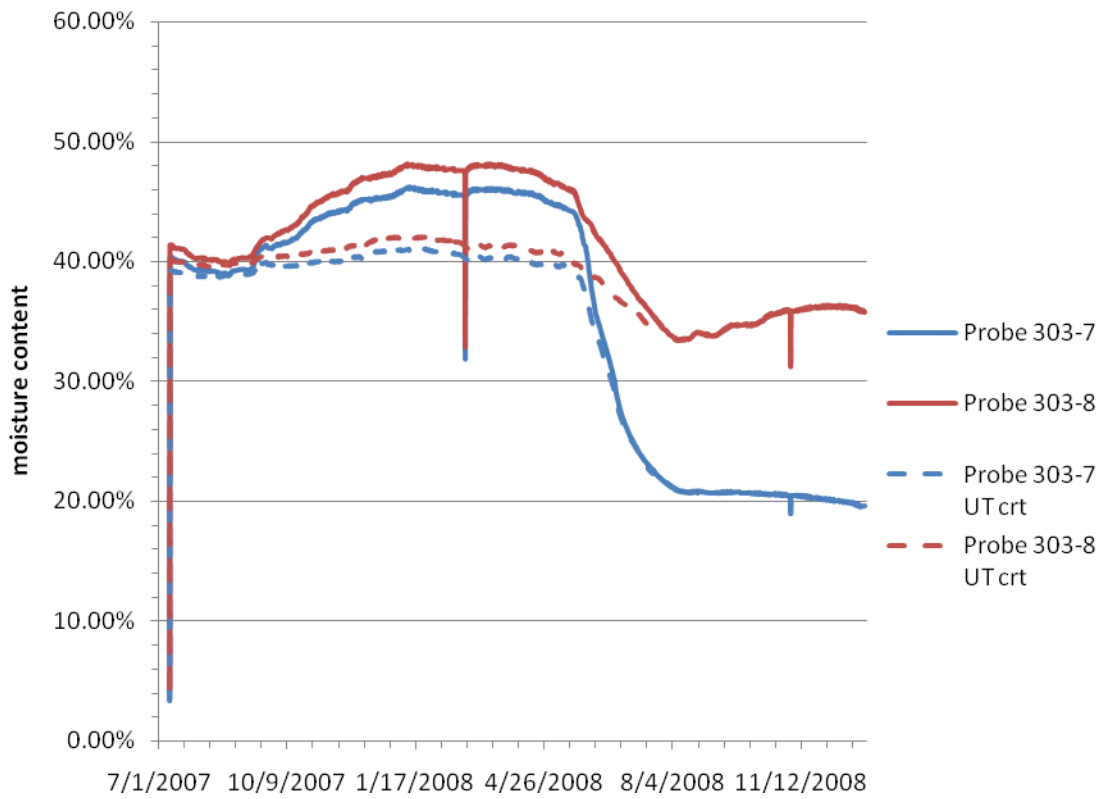


Figure 8.7: A sample comparison of two temperature corrections

Chapter 9: Summary and Conclusions

9.1 SUMMARY OF RESEARCH OBJECTIVES

The purpose of this study is to investigate the effect of soil dry density and temperature on WCR calibration curves. By giving an experimental method that is capable to illustrate the response of WCR sensors in RMA soil using reasonable data interpretation, this study provides better understandings of TDR technique in geotechnical applications.

The objectives of this study stated in Chapter 1 were reached as follow:

- The characteristics of the WCR calibration curve were defined for RMA soil compacted at three different relative compactions, which were 75%, 80%, and 85%. The required water content of the specimen was accessed by two methods: 1) mixing the dry soil particles with calculated water; 2) imposing an inflow that gradually wetted the specimen. The experimental data were fitted using polynomials; these polynomials might be used to predict the moisture content feasibly in applications.
- The responses of WCR sensor in different temperatures were acquired in specimens that were compacted at six different water contents at the relative compaction of 80%. A correction method is studied to translate one response at one random temperature to one response at a standard temperature. This standard temperature is 20 degree Celsius in this research.
- Compared and validated the calibration curves and temperature corrections curves with generic curves provided by manufacturer.

- Applied the results to one field sample that use similar soil with the same dry density.

The tasks for reaching the objectives were completed as follow:

- A literature review was presented to summarize the experimental methods which are usually used to determine the moisture content in soil, the typical parameters that needed to be measured, and the typical calculation equations.
- A background of TDR technique, including the basic physics, a typical circuit, a typical pulse waveform, a layout of typical components, and a typical response wave form, was provided.
- A review of Topp's Equation was presented, which is the most classic responding equation of TDR for monitoring moisture in mineral soil.
- A literature review was presented to summarize the experimental and practical results which were used to characterize and determine the impacts of soil type, soil density, and temperature to the response of TDR probes.
- A sandy lean clay (CL), RMA soil, was chosen to be used in the experiments. The compaction properties as well as the specific gravity of the soil were also investigated.
- A type of low frequency two-rod TDR sensor, Water Content Reflectometer CS-616 (WCR CS-616), was selected to measure the response in RMA soil specimen. The outputs of the sensor were reflecting periods, which were highly related to the moisture content of the material around the sensor.
- Quantitative variables were defined for the deriving the moisture-response relationship, specifically the reflecting period, the time, the density, the temperature and the water content of the specimen. Instrumentations were designed and arranged for measuring these variables: PVC tubes were

manufactured for containing the specimen and providing the environment for moisture equilibrium; an air-pistol compaction hammer were selected to knead the soil to the required density; the temperature stationary environment was found to be controlled well using a plastic cooler; the temperature altering environment was established by coupling a freezer, heating elements, a logic temperature controller and a temperature sensor; the reflecting periods from WCR were captured automatically by a datalogger and a PC. The layout of these instruments permits continuous automatic measurements.

- A theoretical explanation of different stages of WCR signals was presented, which were used to indicate the representative response of WCR.

9.2 CONCLUSION OF REFLECTION CALIBRATION RESULTS

9.2.1 Conclusion of WCR Reflection Results under Varied Relative Compactions

The key findings in investing dry density effect on WCR response are listed as follow:

- The theoretical assumption of the WCR method for measuring soil moisture was proved reasonable. Within all experiments with a given relative compaction, the reflecting periods from the WCR were measured to be positively related the water contents of the specimens. These measurements indicated that WCR responses were governed by the dielectric constant of the medium around, since the dielectric constant of a soil specimen was mainly attributed the its water phase.
- The sensitivity of WCR responses to water content was found to be low at high water content near saturation. Although the volumetric water content increased from 27% to 37%, the increment of reflecting period was not more than 2ms. In

comparison, the increase of reflecting period was approximately 6ms as the volumetric water content increased from 17% to 27%.

- The differences of WCR response curves measured from specimens with different relative compactions indicated the soil particle could impact the response of WCR. Generally, the WCR reflecting period increased as the relative compaction increased (the volume of soil particles in unit space increased). However, soil particles played a less significant role to the changes of WCR responses than water content. This relation indicated soil particles have relatively small dielectric constants to water.
- The method that fitted the experimental results best was found to be Cubic Consolidated Fit and Shifts. The equations are:

$$\theta = 0.285 * 10^{-5} \cdot t^3 - 0.00209 \cdot t^2 + 0.059741 \cdot t + Shift \text{ (Equation 9.1)}$$

$$Shift = -0.2081 * \gamma_d - 0.2132 \text{ (Equation 9.2)}$$

Specific findings in the testing program include:

- Specimen containing setup was observed to be satisfactory. The total weights of the specimen after testing were measured close to the value before testing, indicating that moisture just redistributed in the specimen but did not evaporate to outside of the container.
- The temperature control environment was found to be satisfactorily achieved. Although the temperature in lab could alter from 20 °C to 23°C within one day, the temperature inside the testing cooler was 21.5~22°C.

- The results of WCR responses over time indicate that the transportation of moisture in soil specimen would be ceased after a period of time, reaching the moisture equilibrium stage. For the geometry of specimen tested in this study, the duration for reaching equilibrium stage was usually 40 hours.
- Specifically surface expansions of some specimens were observed. The specimens that were tested using imposing inflow method were observed to expand 6mm to 8mm by the end of testing, where the original specimen length is 320mm.
- WCR measurements from all soil specimens were smaller than that measured in water (43.70ms); moreover, measurements from soil specimens were bigger than that measured in dry air (14.92ms).
- The working quality of WCR sensors were likely stable. The responses in pure water and dry air did not change after four months from the start of the experiments.

9.2.2 Conclusion of Temperature Corrections Results

The key findings in investigating temperature effects on WCR responses are listed follow:

- For each specimen of one given water content, readings measured at higher temperatures yielded a bigger reflecting period; vice versa.
- Drops between reflecting periods measured before and after freezing were observed. These drops were observed to be related to water content; the higher was the water content the more significant was drop. The drop of the driest specimen ($\theta_v = 2.8\%$) was almost negligible. Based on the evidence provided previously that the WCR response might be govern by water content of soil, this

observation indicated a significant decrease of dielectric constant of water after freezing.

- Consistent with the observations from the reflection calibration, for specimens investigated at one given temperature, reflecting periods were found to be positive related to water contents.
- The changing rates of WCR responses with water content were found to be relatively small at negative temperatures compared to at positive temperatures. This observation could have provided further supports to the view that the dielectric constant of water decreased significantly after freezing, meaning that the influence of water to WCR responses was weakened.

Specific findings in the testing program include:

- The temperature control setup was acceptably attained. Thirteen temperatures, ranging from 40°C to -20°C with a 5°C decrement, were achieved inside the testing freezer. The error of the temperature setup was found to be 1°C.
- The measurements from WCR over time were observed to be stable after approximately 20-24 hours after a temperature change in the freezer. These readings at stable stages were selected to represent the WCR responses at the temperatures.
- The reflecting period, water content and temperature profile attained in the study show similar trend to the results presented by Benson and Wang (2002).

9.3 SUGGESTIONS FOR FUTURE RESEARCH

Recommendations of future study include:

- Improve the calibration and interpretation of WCR responses. The WCR response curves could be improved by adding additional data points from specimen with different relative compactions and water contents. Further study could extend the range of relative compaction selected, so that the impact of soil density could be quantified.
- Refine the WCR responses, temperature and water content relation. Especially, the temperature correction database below the freezing point could be enhanced. Since the impact of water to WCR responses below the freezing point is weakened, the influence of soil type and soil density would be strengthened. Studying these influences might extend our understandings of soil.
- Examine the effects of freeze/thaw cycle and hysteresis. Drops of the WCR response were observed when temperature decrease to below freezing point. However, the effect of thawing is still unknown. Quantify a relation of freeze/thaw effect might greatly enhance the applications of WCR in long term field investigation in cold region.
- Develop an approach of using WCR as a density indicator. Since there is a known relationship of responses, density and water content, by coupling of other water content sensors, WCR could also be applied as a non-destructive alternative technique for measuring soil density.

References

- ASTM D422. 2007. "Standard Test Method for Particle-Size Analysis of Soils." The American Society for Testing and Materials. West Conshohocken, PA.
- ASTM D698. 2007. "Standard Test Methods for Laboratory Compaction Characteristics of Soil Using Standard Effort (12 400 ft-lbf/ft³ (600 kN-m/m³))." The American Society for Testing and Materials. West Conshohocken, PA.
- ASTM D854. 2006. "Standard Test Methods for Specific Gravity of Soil Solids by Water Pycnometer." The American Society for Testing and Materials. West Conshohocken, PA.
- ASTM D2487. 2006. "Standard Practice for Classification of Soils for Engineering Purposes (Unified Soil Classification System)." The American Society for Testing and Materials. West Conshohocken, PA.
- ASTM D4318. 2005. "Standard Test Methods for Liquid Limit, Plastic Limit, and Plasticity Index of Soils." The American Society for Testing and Materials. West Conshohocken, PA.
- Benson, C. H., and Wang, X. 2006. "Temperature-Compensating Calibration Procedure for Water Content Reflectometers" TDR 2006. Purdue University, West Lafayette, Indiana. September 18-20, 2006.
- Blonquist, J., Jones, S., and Robinson, D. 2005. "Standardizing Characterization of Electromagnetic Water Content Sensors: Part2. Evaluation of Seven Sensing Systems." *Vadose Zone J.*, 4, pp. 1059-1069.
- Campbell Scientific, Inc. 2002. "Instruction Manual: CS616 and CS625 Water Content Reflectometers." Logan: Campbell Scientific, Inc.
- Cataldo, A., Vallone, M., Tarricone, L., and Attivissimo, F. 2008. "An Evaluation of Performance Limits in Continuous TDR Monitoring of Permittivity and Levels of Liquid Materials." *Measurement*, 41 (2008) 719-730.
- Chandler, D. G., Seyfried, M., Murdock, M., and McNamara, J. P. 2004. "Field Calibration of Water Content Reflectometers." *Soil Sci. Soc. Am. J.* 68 (2004), pp.1501-1507.
- Friedman, S. P., Jones, S. B., and Robinson, D. A. 2006. "Review of Geometrical and Interfacial Factors Determining the Effective Permittivity-Volumetric Water

- Content Relationships of Soils and Rocks.” TDR 2006. Purdue University, West Lafayette, Indiana. September 18-20, 2006.
- Kelleners, T. J., Seyfried, M. S., Blonquist, J. M., Bilskie, Jr., J., and Chandler, D. G. 2005. “Improved Interpretation of Water Content Reflectometer Measurements in Soils” *Soil Sci. Soc. Am. J.* 69 (2005), pp. 1684-1690.
- Kim, K. C., and Benson, C. H. 2002. “Water Content Reflectometer Calibrations for Final Cover Soils.” Geo Engineering Report No. 02-12, the University of Wisconsin-Madison, Madison, WC.
- Ledieu, J., De Ridder, P., and Dautrebande, A. 1986. “A Method for Measuring Soil Moisture by Time Domain Reflectometry.” *J. Hydrology*, Vol.88, 1986, pp. 319-328.
- Logsdon, S. 1994. “Calibrating TDR with Undisturbed Soil Cores for TDR Use in Monitoring Subsurface Lateral Water Flow.” U.S. Bureau of Mines, Special Publication SP 19-94, NTIS PB95-105789, pp. 269-280.
- McCartney, J. S. 2007. “Determination of the Hydraulic Characteristics of Unsaturated Soils using a Centrifuge Permeameter.” Dissertation, the University of Texas at Austin, Austin, TX.
- O’Connor, K. M., and Dowding, C. H. 1999. “GeoMeasurements by Pulsing TDR Cables and Probes.” Boca Raton: CRC Press.
- Petersen, L. W., 1995. “Sampling Volume of TDR Probes Used for Water Content: Practical Investigation” Paper in the Proceedings of Symposium: Time-Domain Reflectometry Applications in Soil Science, SP Report No.11, June 1995, Vol. 3, pp. 57-62.
- Pozzato, A., Tarantino, A., McCartney, J., and Zornberg, J. 2008. “Use of TDR to Evaluate the Effect of Dry Density on the Relationship between Water Content and Apparent Dielectric Permittivity of Compacted Clays.” First European Conference on Unsaturated Soils. July 3-5. Durham, UK.
- Seyfried, M. S., and Murdock, M. D. 2004. “Measurement of Soil Water Content with a 50-MHz Soil Dielectric Sensor” *Soil Sci. Soc. Am. J.* 68 (2004), pp. 394-403.
- Topp, G. C., Davis, J. L., and Annan, A. P. 1980. “Electromagnetic Determination of Soil Water Content: Measurements in Coaxial Transmission Lines.” *Water Resources Research*, Vol.16, No.3, pp. 574-582.
- Zakri, T., Laurent, J. -P., and Vauclin. M. 1998. “Theoretical Evidence for Lichtenecker’s Mixture Formulae Based on The Effective Medium Theory.” *Journal of Physics D: Applied Physics*, 31, pp. 1589-1594.

Vita

Yucao Tang is the son of Weishan Tang and Meiqun Yu. Yucao was born in Guangzhou, China on March 5, 1985. Yucao attended Guangzhou No.2 middle school, and graduated in July 2003. Yucao attended Tsinghua University at Beijing in August 2003 to July 2007, and received BS degree in Hydraulic Engineering. From Aug 2007, Yucao attended the University of Texas at Austin, pursuing a MS degree in civil engineering.

Permanent address: 67 Nan'an Rd, A3-2101, Guangzhou, Guangdong, China. 510160

This thesis was typed by Yucao Tang.